frontiers in Forests and Global Change

TYPE Original Research
PUBLISHED 10 April 2026
DOI 10.3389/ffgc.2026.1783866

OPEN ACCESS

EDITED BY
Xiankai Lu,
Chinese Academy of Sciences (CAS), China

REVIEWED BY
Jihui Tian,
South China Agricultural University, China
Xiang Zhang,
Nankai University, China

*CORRESPONDENCE
Robert Mikutta
✉ robert.mikutta@landw.uni-halle.de

RECEIVED 08 January 2026
REVISED 04 March 2026
ACCEPTED 10 March 2026
PUBLISHED 10 April 2026

CITATION
Mikutta R, Mikutta C, Boy J, Degenhardt D, Dormann G, Guggenberger G, Joergensen RG, Craighero A, Schulz S, Spohn M, Vázquez E and Andrino A (2026) Soil phosphorus scarcity promotes *in-situ* abiotic and microbial mobilization of iron oxide-bound phosphorus. *Front. For. Glob. Change* 9:1783866. doi: 10.3389/ffgc.2026.1783866

Soil phosphorus scarcity promotes *in-situ* abiotic and microbial mobilization of iron oxide-bound phosphorus

Robert Mikutta[1]*, Christian Mikutta[2], Jens Boy[3], Dustin Degenhardt[3], Gabriele Dormann[4], Georg Guggenberger[3], Rainer Georg Joergensen[4], Alexandra Craighero[5,6], Stefanie Schulz[5], Marie Spohn[7], Eduardo Vázquez[8] and Alberto Andrino[3]

[1]Soil Science and Soil Protection, Institute of Agricultural and Nutritional Sciences, Martin Luther University Halle-Wittenberg, Halle (Saale), Germany, [2]Soil Mineralogy, Institute of Earth System Sciences, Leibniz University Hannover, Hannover, Germany, [3]Section Soil Science, Institute of Earth System Sciences, Leibniz University Hannover, Hannover, Germany, [4]Department of Soil Biology and Plant Nutrition, University of Kassel, Witzenhausen, Germany, [5]Research Unit Comparative Microbiome Analysis, Helmholtz Zentrum München, German Research Center for Environmental Health, Neuherberg, Germany, [6]Chair of Terrestrial Ecology, Technische Universität München, Freising, Germany, [7]Department of Soil and Environment, Swedish University of Agricultural Sciences, Uppsala, Sweden, [8]Department of Agricultural Production, Universidad Politécnica de Madrid, Madrid, Spain

In temperate forest ecosystems, phosphorus (P) leached into the mineral soil largely adsorbs to pedogenic iron (Fe) and aluminum (Al) oxides. This raises the question as to which extent adsorbed P in mineral soil can be recycled and whether soil P scarcity promotes microbial communities better adapted to use these P sources. To investigate the mobilization of P bound to hydrous Fe oxides under natural conditions, goethite with adsorbed orthophosphate (OP) and phytic acid (PA) was buried for 35 months in beech (*Fagus sylvatica*) forest soils at three sites in Germany varying in geogenic P supply. We quantified total and surface P losses by X-ray fluorescence spectrometry and photoelectron spectroscopy and assessed changes in bioavailable P by sequential extractions (resin and $NaHCO_3$). Surrounding soil and goethite samples were analyzed for amino sugars, acid phosphomonoesterase activity, and microbial metagenomic properties. Total losses of OP and PA ranged between 1% and 58%, with lower losses of PA due to stronger sorption complexes. Resin- and $NaHCO_3$-extractable P declined by 48%–94% and 31%–75%, respectively. Besides P desorption caused by concentration gradients, microbial P mining explained higher P losses under soil P scarcity. Based on stocks of P bound to pedogenic Fe and Al oxides, mineral P saturation levels, and *in-situ* P release rates, we infer that oxide-bound P in a P-poor sandy soil could likely not meet the P requirement of the vegetation, despite higher P losses. This result supports the

idea that vegetation under P-deficient conditions depends more on P recycling in forest floor layers than under conditions of high P availability. Conversely, at the loamy P-rich sites, release of P bound to Fe and Al oxides was high enough to contribute to forest nutrition. Our results indicate that P, especially OP, when leached into mineral soil and sorbed to Fe and Al oxides, is not fully passivated but partly recycled at high P saturation levels, thus contributing to biological assimilation or downward P translocation.

KEYWORDS

beech forest, iron oxide, orthophosphate, phosphorus nutrition, phytate

Introduction

Phosphorus (P) is a key nutrient element for plants and microorganisms, occurring in soil in a variety of inorganic and organic compounds, including orthophosphate, condensed phosphates, organic P esters, and phosphonates (Turner et al., 2007; Lang et al., 2017; Yan et al., 2023). It is well established that soil development over time results in diminishing P contents, especially those contained in primary minerals like apatite (Walker and Syers, 1976). This results in relatively more P contained in organic matter (OM) or bound to secondary minerals such as iron (Fe) and aluminum (Al) oxides (Richardson et al., 2004; Brucker and Spohn, 2019). The high ability of P compounds to sorb to reactive minerals (Spohn, 2024) can at least transitionally limit biological processes (Vitousek et al., 2010). A declining soil P availability reduces plant productivity (Richardson et al., 2004) and changes the soil microbiome toward more demand-driven acquisition strategies (Oliverio et al., 2020). These ecosystem patterns collectively merged into a conceptual framework for P nutrition in forest ecosystems, linking soil P availability to the strategies of plants and soil organisms involved in P cycling (Lang et al., 2017). According to this framework, plants and soil organisms in young, P-rich soils are supposed to mobilize P mainly from primary minerals like apatite, and P losses are high ("open P cycle"). In contrast, under P-poor conditions, plants and microorganisms are supposed to mainly meet their P demands by recycling of organic sources (forest floor and soil horizons rich in OM), and P losses are rather low ("tight P cycle").

In P-poor systems, soil organisms are hypothesized to be better adapted to nutrient acquisition from "hard-to-exploit" P sources, like P adsorbed to Fe and Al oxides. Especially, mycorrhizal fungi are advocated as key players in mobilizing mineral-bound P. Laboratory greenhouse experiments demonstrated the ability of mycorrhizal associations to mobilize and use P from different adsorbed P sources. For example, it was shown that arbuscular mycorrhizal fungi (*Solanum lycopersicum* × *Rhizophagus irregularis*) transferred up to 6% of P from goethite-adsorbed orthophosphate (OP) and phytic acid (PA) to the host plant over a period of 90 days (Andrino et al., 2019). Acquisition from adsorbed P compounds went along with a larger assimilate-C investment of plants compared to treatments with dissolved P compounds. The presence of low-molecular-weight carboxylic acids suggests that mobilization of goethite-bound P was driven by mineral dissolution and surface exchange reactions (Andrino et al., 2021). Results further showed a larger mobilization of OP than PA, the latter resembling P-monoesters with multiple phosphate groups (Darch et al., 2014), forming strong bonds to mineral surfaces (Spohn, 2024). In addition, PA must be enzymatically hydrolyzed before P becomes available to plants (Li et al., 1997). More recently, Amadou et al. (2022) showed in a greenhouse experiment that 3%–18% of P derived from mineral-adsorbed organic P (PA, glucose-6-phosphate, glycerophosphate) was taken up by ryegrass (*Lolium multiflorum*), a plant with symbiotic arbuscular mycorrhizal fungi. Unlike for arbuscular mycorrhiza, the contribution of ectomycorrhizal fungi to P resource partitioning still remains unclear. Employing ^{33}P-labeling, Schreider et al. (2022) showed that also ectomycorrhizal associations of gray poplar (*Populus x canescens* × *Paxillus involutus*) were able to utilize up to 5% of different, simultaneously applied P sources within 108 days. More P from dissolved OP, adenosine monophosphate, and apatite than goethite-bound OP was taken up by the host plant. This finding aligns with results of another mesocosm experiment utilizing ectomycorrhized beech plants (*Fagus sylvatica*) grown in a P-poor subsoil amended with goethite-adsorbed OP and PA. At the end of the experiment, total P contents in plants indicated the inability of beech to acquire P from goethite surfaces within two vegetation periods (Klotzbücher et al., 2020).

While there is scattered evidence from greenhouse experiments that mineral-bound inorganic and organic P compounds can to some extent be utilized by plant-microbe associations, it is still unclear how these results can be transferred to natural conditions, especially with regard to soils with ectomycorrhizal associations. D'Amico et al. (2020) exposed mesh bags filled with goethite-bound OP or PA for 13 months to the organic layer-mineral soil interface in P-poor soils of the Italian Alps. The P release far exceeded that observed in greenhouse experiments, reaching 65% for OP and 45% for PA. The high mobilization was mainly attributed to ectomycorrhizal activity, though it might have been promoted by exchange reactions with percolating dissolved organic matter (DOM), as mesh bags were installed directly underneath organic layers where DOM fluxes are typically high (Leinemann et al., 2016). To this end, we currently lack further field studies exploring P mobilization from adsorbed P sources in mineral soil, especially in deeper soil horizons. It remains unclear how relevant P mobilization from mineral-bound sources is for forest nutrition, also in comparison to other P sources like forest floor layers.

In this study, we present a field experiment, where goethite-bound OP and PA were exposed for 35 months to forest soils under beech along a soil P availability gradient, which was comprehensively investigated as part of the German priority programme SPP 1685 "Ecosystem Nutrition: Forest strategies for limited phosphorus resources" (Lang et al., 2017). Specifically, we were interested to which extent P adsorbed to goethite, which is by far the most abundant Fe oxide in temperate soils (Cornell and Schwertmann, 2003), is mobilized along the soil P gradient in topsoil and subsoil horizons and how mobilization of adsorbed P relates to specific soil properties, microbial accumulation patterns, and enzyme activities. Besides total P losses from goethite, we quantified P release from goethite surfaces using X-ray photoelectron spectroscopy and losses of potentially bioavailable P fractions (resin- and $NaHCO_3$-extractable P). We additionally assessed the accumulation of organic carbon (OC) as well as acid phosphomonoesterase activity, microbial abundancies, and amino sugars as microbial marker compounds in mesh bags and surrounding soil. Water-extractable OC and organic N in soil directly in contact with the mesh bags served as proxy for DOM that could potentially exchange with adsorbed P. Based on P stocks associated with secondary minerals and observed P release rates, we discuss the potential relevance of mineral-bound P for forest nutrition. We hypothesized that (i) irrespective of the soil P status, adsorbed P becomes mobilized, with OP being released at a higher rate than PA, (ii) increasing soil P scarcity promotes the mobilization of oxide-bound P by microbial and especially fungal activity, and (iii) release of adsorbed P occurs at rates quantitatively relevant for forest nutrition.

Materials and methods

Preparation of goethite-phosphorus associations and mesh bags

Goethite was loaded with OP and PA as described in Klotzbücher et al. (2020), using well-crystalline goethite (Bayferrox 920 Z, Lanxess) with a specific surface area of 20.4 $m^2\ g^{-1}$ as determined by N_2 gas adsorption (BET method). Briefly, solutions containing 1 g P L^{-1} were prepared using KH_2PO_4 or K-phytate and pH was adjusted to 4.0 using HCl or KOH. This pH value corresponded to the acidic conditions of the soils examined (Table 1) and ensured the uptake of suitable amounts of P for the field exposure experiment described below. Goethite was reacted for 16 h with P solutions at a solid-to-solution ratio of 1:8 (w/v). The solids were separated from solution by centrifugation at 8,200 × *g* for 45 min at 5 °C and washed with ultrapure water until the electric conductivity of washing solutions was <100 µS cm^{-1}. The goethite-P associations were frozen at −20 °C, freeze-dried, homogenized, and sieved to <250 µm. Mesh bags for field exposure consisted of a round, open plastic lid that contained a mesh bag filled with pure goethite or P-loaded goethite (Figure 1). The polyamide gaze (PA-20/14, Franz Eckert GmbH) used for the mesh bags had a mesh size of 20 µm and prevented access of plant roots. The mesh bags were filled with pure goethite (GOE, 11.0 g), OP-loaded goethite (GOE-OP, 12.3 g), and PA-loaded goethite (GOE-PA, 9.7 g), so that the total P content was similar in both P treatments (∼18 mg). Additionally, 0.2 g ZrO_2 was added to each mesh bag in order to quantify potential goethite losses under field conditions via decreasing Fe/Zr ratios.

Study sites, field exposure, and sampling

The field exposure experiment was conducted in three even-aged beech (*Fagus sylvatica* L.) forests located across Germany: Bad Brückenau (BBR, 5579975 N; 3566195 E), Mitterfels (MIT, 5426906 N; 4564502 E), and Lüss (LUE, 5857057 N; 3585473 E) (Lang et al., 2017; Müller et al., 2020). Site characteristics including general soil properties are reported in Table 1. In spring 2018, six mesh bags of each treatment (GOE, GOE-OP, GOE-PA) were installed along a ∼5 m wide trench in mineral topsoil (5 cm depth) and subsoil (30 cm depth) (Figure 1). After *in-situ* incubation for 35 months, mesh bags were excavated in April 2021, cleaned of adhering soil material, and transported on refrigerated ice packs to the laboratory. Additionally, we collected soil material directly above each mesh bag (∼5 cm). Half of the mesh bags and soils was air-dried at 30 °C for element analyses, while the other half was kept at −25 °C and field-moist for microbial and enzyme activity analyses. The dry weight of goethite and soil samples was determined gravimetrically upon drying at 105 °C.

General properties of soils and goethite samples

Total C and N contents of soils and goethites were determined by dry combustion (Vario MAX Cube, Elementar Analysensysteme). As the soil pH was strongly acidic (Table 1) and P-loaded goethites were prepared at pH 4, total C corresponded to OC. Soil pH was measured potentiometrically in 0.01 M $CaCl_2$ solution at a solid-to-solution ratio of 1:2.5 (w/v). Water-extractable OC (WEOC), total N (WETN), and inorganic N (N_{min}) in soils above mesh bags were extracted in 40 mL ultrapure water from 8 g soil. Suspensions were shaken for 1 min (50 agitations), left for 18 h in the dark at 20 °C, and centrifuged for 10 min at 2,900 × *g*. Supernatants were filtered through 0.45 µm polyethersulfone membranes (Supor®) and OC and total N (TN) concentrations in the filtrates determined with a multi N/C® 3100 analyzer (Analytik Jena AG). Concentrations of N_{min} (NO_3^- + NH_4^+) were analyzed using a Continuous Flow Analyzer (ScanPlus, Skalar Analytical B.V.). WEON was calculated by TN − N_{min}.

Phosphorus associated with pedogenic minerals

Mineral horizons (<2 mm fine earth fraction) sampled within the top 30 cm of soil pits (Lang et al., 2017) were sequentially extracted by acid ammonium oxalate (AAO) at pH 3 (Carter and Gregorich, 2008) and dithionite-citrate-bicarbonate (DCB) (Blakemore et al., 1987). The amount of P co-released with Fe and Al was determined after ultracentrifugation (300,000 × *g*, 6 h) by inductively coupled plasma–optical emission spectrometry (ICP-OES) (Varian 725-ES, Varian). Acid oxalate extracts Fe, Al,

TABLE 1 Location and properties of soils at the study sites Bad Brückenau (BBR), Mitterfels (MIT), and Lüss (LUE) under dominant *Fagus sylvatica* vegetation.

	Unit	BBR		MIT		LUE	
Location		Bavarian Rhön		Bavarian Forest		Lower Saxon Plain	
Altitude	m (a.s.l.)	809		1023		115	
MAP	mm	1031		1299		779	
Parent material		Basalt		Paragneis		Glacial till	
Soil type		Dystric Skeletic Cambisol		Hyperdystric Chromic Folic Cambisol		Hyperdystric Folic Cambisol	
Texture topsoil		Silty clay loam		Loam		Loamy sand	
Texture subsoil		Loam		Sandy loam		Sand	
Age of stand (2018)	a	138		132		133	
Total soil P stock (1 m)	g m^{-2}	904		678		164	
Resin-P (0–5 cm)	mg kg^{-1}	116		70		11	
		Soil around mesh bags installed at different depths					
		5 cm	30 cm	5 cm	30 cm	5 cm	30 cm
pH ($CaCl_2$)	(−)	3.7	4.0	3.4	3.9	2.9	4.0
		(0.1)	(0.0)	(0.2)	(0.1)	(0.1)	(0.1)
OC	g kg^{-1}	95.3	86.0	61.7	53.4	18.3	13.2
		(15.0)	(16.9)	(14.8)	(13.2)	(4.2)	(5.0)
TN	g kg^{-1}	7.5	6.7	3.8	3.2	0.8	0.6
		(1.4)	(1.4)	(1.0)	(1.0)	(0.2)	(0.2)
TP	mg kg^{-1}	2856	3030	1116	1038	103.3	121.1
		(146)	(83)	(72)	(47)	(26.2)	(5.7)
WEOC	mg kg^{-1}	456.9	181.0	389.9	147.5	265.6	106.1
		(155.3)	(57.0)	(81.0)	(25.6)	(36.9)	(27.2)
WEON	mg kg^{-1}	57.9	17.0	37.8	14.7	15.9	6.4
		(14.2)	(4.4)	(6.1)	(3.4)	(3.0)	(1.9)
WEOC/WEON	(−)	7.9	10.6	10.3	10.3	16.9	16.7
		(2.4)	(1.5)	(1.0)	(1.5)	(1.7)	(1.4)
N_{min}	mg kg^{-1}	42.7	9.1	21.5	5.9	2.2	0.9
		(14.2)	(5.0)	(7.0)	(6.1)	(1.2)	(0.4)
GalN	µmol g^{-1}	3165	2667	3068	2239	1054	414.0
		(1682)	(1322)	(530)	(461)	(532)	(91.4)
GlcN	µmol g^{-1}	4143	3242	5510	3600	3004	1079
		(2413)	(1674)	(448)	(735)	(935)	(134)
MurA	µmol g^{-1}	249.8	394.2	383.0	329.1	58.7	46.3
		(185.2)	(184.1)	(80.4)	(91.3)	(21.0)	(13.9)
Total AS	µmol g^{-1}	7589 (4255)	7154 (2379)	8961 (982)	6168 (1282)	4117 (1454)	1539 (176)
Total AS/soil OC	(−)	0.86	1.15	1.53	1.66	2.48	1.60
F/B	(−)	2.80	0.85	1.84	1.31	7.49	3.40
		(1.65)	(0.21)	(0.40)	(0.16)	(2.21)	(1.30)
phoD copies	g^{-1}	3.1E+07	1.3E+07	9.1E+06	1.1E+07	7.0E+07	1.0E+08
		(1.4E+07)	(5.1E+06)	(2.8E+06)	(3.5E+06)	(4.6E+07)	(5.4E+07)
gcd copies	g^{-1}	6.6E+06	3.7E+06	4.3E+06	4.3E+06	3.5E+07	1.6E+07
		(4.6E+06)	(3.0E+06)	(2.4E+06)	(4.4E+06)	(2.8E+07)	(1.3E+07)

Values in parentheses refer to standard deviation. MAP, mean annual precipitation; OC, organic carbon; TN, total nitrogen; TP, total phosphorus; WEOC and WEON, water-extractable organic carbon and nitrogen; N_{min}, inorganic nitrogen; GalN, GlcN, and MurA, galactosamine, glucosamine, and muramic acid; AS, amino sugars; F/B, fungal-to-bacterial C ratio. General site and soil properties were taken from Lang et al. (2017).

10.3389/ffgc.2026.1783866

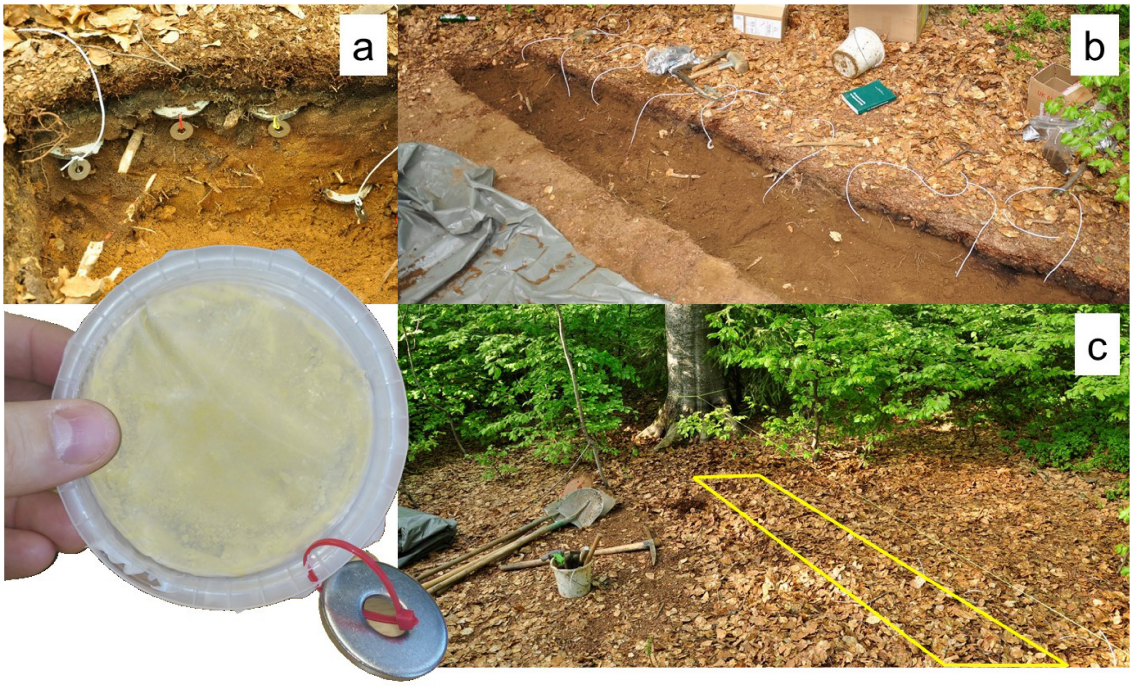

FIGURE 1
Mesh bag filled with goethite before soil exposure (down left) and installation of mesh bags **(a)**. Care was taken to ensure intimate contact between mesh bags and surrounding soil. Mesh bags were installed along a trench with a plastic cord attached to each bag to ease recovery **(b)**. After insertion, soil trenches were closed with excavated soil material, ensuring the same horizon sequence as in the undisturbed soil **(c)**.

and P (Fe/Al/P_{AAO}) primarily from short-range order minerals, but also liberates P from other mineral sources due to the competitive exchange with oxalate. The DCB solution then reductively dissolves the remaining crystalline Fe oxides, thereby releasing associated P (P_{DCB}) together with P forms that are liberated under the more alkaline extraction pH in presence of citrate. As apatite was not abundant in the upper horizons of the studied soils (Stahr et al., 2018; Rodionov et al., 2020), the sum of P_{AAO} and P_{DCB} serves as proxy for P associated with secondary minerals. Based on bulk density of the fine earth fraction and horizon thickness, we calculated P stocks associated with secondary minerals and compared them with total P stocks.

Total element contents of soils and goethite samples

The total element content of soils and goethites before and after field exposure was determined by wavelength-dispersive X-ray fluorescence spectrometry using a S8 Tiger instrument (Bruker AXS). For analysis, fused beads were prepared by mixing ~1 g of solid with 8 g of lithium tetraborate 66%/lithium metaborate 34%. The mixtures were fused in an automated electric fusion machine (XrFuse 6, XRF Scientific Ltd.). Fluorescence spectra were evaluated by the Quant-Express method by accounting for the loss on ignition. Detected elements summed up to 100.0% ± 6.9% (mean ± SD) for soils and 99.3% ± 1.4% for goethite samples, respectively.

Chemical surface composition of goethite samples

The chemical surface composition of goethites before and after field exposure was evaluated by X-ray photoelectron spectroscopy using an AXIS Supra instrument (Kratos Analytical) equipped with an Al Kα source. Samples were mounted on adhesive Cu-Ni tape and survey spectra (0-1200 eV) were recorded at three randomly selected spots of 300 µm × 700 µm in the hybrid lens mode with an emission current of 15 mA and a step size of 1 eV, with up to five sweeps employing a pass energy of 160 eV. To quantify the surface P loss, detail scans were recorded in the P 2p-Fe 3s region (79-144 eV) using a pass energy of 160 eV, an emission current of 15 mA, and a step size of 0.1 eV with up to seven sweeps. A contribution of Mg 2s peaks to the Fe 3s region was excluded based on missing Mg KLL lines in survey spectra and supported by undetectable Mg in X-ray fluorescence spectra. The P 2p-Fe 3s region of GOE control samples are exemplarily shown in Supplementary Figure 1. Binding energies of survey and detail spectra were charge-corrected based on C 1s signals measured under identical conditions and set to 285.0 eV. All spectra were evaluated using the ESCApe software (Kratos Analytical, Version 1.4) and element contents were quantified using the respective element sensitivity factors. The P 2p-Fe 3s spectra were evaluated by integrating the P 2p and Fe 3s region using a Shirley background function in order to calculate the surface P/Fe ratio based on the obtained P and Fe at% values.

Scanning electron microscopy

Selected goethite samples were examined by scanning electron microscopy with a TESCAN CLARA instrument equipped with secondary and backscatter electron detectors. Samples were mounted on stubs with adhesive C tape and sputter-coated with C to increase electric conductivity. For imaging, the acceleration voltage was set to either 1.0 or 7.5 keV and beam currents to 15 or 75 pA, respectively.

Mobilizable phosphorus fractions in goethite samples

Phosphorus-loaded goethites were sequentially extracted at room temperature before and after field exposure to account for changes in mobilizable P as described in Klotzbücher et al. (2019). Briefly, 0.5 g goethite together with two strips (9 mm × 62 mm) of an anion exchange resin in HCO_3^- form (551642S, VWR) were shaken in 30 mL ultrapure water for 16 h. Phosphorus from the recovered resin strips was extracted with 20 mL of 0.5 M HCl for 16 h. After removal of resin strips, suspensions were centrifuged (25,000 × *g*, 10 min), supernatants decanted, and the samples resuspended into 30 mL 0.5 M $NaHCO_3$ solution (pH 8.5). After shaking for 16 h, suspensions were centrifuged (25,000 × *g*, 10 min) and supernatants filtered through 0.45-µm polyethersulfone membranes. Phosphorus concentrations in the filtrates were determined by ICP-OES (Ultima 2, Horiba Jobin-Yvon). Resin-extractable P (P_{resin}) represents weakly bound P readily desorbable into P-undersaturated solutions, while $NaHCO_3$-extractable P (P_{bicarb}) accounts for P exchangeable with (in)organic anions.

Amino sugar analyses

Amino sugars in soil and goethite samples were determined according to Appuhn et al. (2004) as described in Indorf et al. (2011). Samples were weighed into hydrolysis flasks and hydrolyzed in 10 mL of 6 M HCl at 105 °C for 6 h. Hydrolyzates were purified at 40 °C using rotary evaporators (Laborota 4000 efficient, Heidolph). Residues were re-dissolved twice in 1 mL ultrapure water and evaporated, and finally transferred to 1.5-mL Eppendorf vials. After centrifugation at 15,700 × g for 10 min, supernatants were analyzed by high-performance liquid chromatography. Pre-column sample derivatization was performed with ortho-phthaldialdehyde in a Dionex Ultimate WPS-3000TSL analytical autosampler with in-line split-loop injection and thermostat, coupled to an Ultimate 3000 pump and an Ultimate 3000 fluorescence detector set at 330 nm excitation and 445 nm emission wavelengths. Chromatographic separation was carried out using a precolumn [SecurityGuard Cartridge C18 2 × (4 × 2 mm ID, Phenomenex AJO-4286)] and a main column [SphereClone 5 µm ODS (2) 150 × 4.6 mm 80 Å, Phenomenex 00F-4144-EO]. The sum of glucosamine, galactosamine, and muramic acid was used as an approximate value for the total amino sugar content. Following established methodology, we used amino sugars as biomarkers for microbial necromass. Fungal chitin (N-acetylglucosamine) is the main source of glucosamine in soil, whereas muramic acid is exclusively derived from the peptidoglycan of bacterial cell walls, particularly those of Gram-positive bacteria (Joergensen, 2018; Hu et al., 2024). In contrast, galactosamine is a component of extracellular polymeric substances formed during fungal and bacterial growth (Oliva et al., 2024, 2025). Based on fungal glucosamine and bacterial muramic acid contents, we calculated the fungal-to-bacterial C ratio (F/B) (Appuhn and Joergensen, 2006) as a proxy for the relative contribution of fungi to the microbial community colonizing goethite surfaces and the surrounding soil. Based on F/B ratios, we tested whether fungal-dominated communities are associated with enhanced P release from goethite.

Quantitative real time PCR of marker genes in soil and goethite samples

SYBR Green-based quantitative real-time PCR (qPCR) assays were performed on a 7300 Real-time PCR System (Thermo Fisher Scientific). For the absolute abundances of bacteria, the 16S rRNA gene was targeted using the primer pairs FP16S (5′-GGTAGTCYAYGCMSTAAACG-3′) and RP16S (5′-GACARCCATGCASCACCTG-3′) (Bach et al., 2002) and the 16S rRNA gene from *Pseudomonas putida* as a standard. To determine the absolute abundance of fungi the Internal Transcribed Spacer (ITS) region was targeted using the primer pairs ITS1 (5′-TCCGTAGGTGAACCTGCGG-3′) and ITS4 (5′-TCCTCCGCTTATTGATATGC-3′) (White et al., 1990) and the ITS region of *Fusarium* spec. as a standard. As alkaline phosphatase genes (*phoD*) have been detected in the acidic forest soils studied (Bergkemper et al., 2016), we determined the abundance of P-mineralizing bacteria by targeting *phoD* as described in Bergkemper et al. (2016), using the *phoD* gene from *Bradyrhizobium japonicum* as standard. To quantify the absolute abundance of P-solubilizing bacteria, the Quinoprotein glucose dehydrogenase gene *gcd* was targeted, using *Salmonella enterica* DSM 17058 as standard source (Bergkemper et al., 2016). The four standards were cloned into pCR® -Blunt Vector (Zero Blunt™ PCR Cloning Kit, Thermo Fisher Scientific) and a dilution series of 10^2–10^8 was used in the qPCR. To exclude any inhibitory effect of co-extracted humic substances, a preliminary sample dilution test was performed, which revealed 1:64 as the ideal dilution. The final qPCR reaction mixtures of 25 µL contained 12.5 µL SYBR Green PCR Master Mix (Thermo Fisher Scientific), 10 pmol of each primer (Metabion), 0.5 µL 3% bovine serum albumin (Sigma), 8.5 µL diethylpyrocarbonate-treated water, and 2 µL DNA template or again 2 µL diethylpyrocarbonate-treated water for the negative control. All amplifications in the qPCR cycler started with an initial denaturation step at 95 °C for 10 min. The thermal profile for the 16S rRNA gene amplification was as follows: 95 °C for 45 s (denaturation), 58 °C for 45 s (annealing), and 72 °C for 45 s (elongation) for 40 cycles. The ITS thermal profile started with 94 °C for 30 s (denaturation), 53 °C for 30 s (annealing), and 72 °C for 45 s (elongation). The *phoD* amplification program started with 5 cycles touchdown with 95 °C for 15 s (denaturation), 65 °C for 1 min (annealing), and 72 °C for 1 min (elongation) followed by 40 cycles with 60 °C annealing temperature. To confirm the specificity of the amplicons after each PCR run, a melting curve analysis and an agarose gel was prepared. R^2 values for all genes were >0.99. The amplification efficiencies (Eff), calculated with $Eff = -1 + 10^{(-1/slope)}$, were 78%–82% for 16S rRNA, 70%–74% for ITS, 76%–86% for *phoD*, and 63%–65% for *gcd*. We also

measured *phoN* (acid phosphatase), *appA* (phytase), and *phnX* (phosphonatase) genes, but these remained below quantification levels in all goethite samples.

Phosphomonoesterase activity in soil and goethite samples

Potential acid phosphomonoesterase activity was determined according to Tabatabai and Bremner (1969), with the reaction termination step modified following Margenot et al. (2018). Briefly, 1 g of soil or 0.5 g of exposed goethite was incubated in duplicate with 1 mL of 50 mM p-nitrophenyl phosphate and 4 mL of modified universal buffer (pH 6.5) at 37 °C for 1 h. After incubation, the reaction was terminated by adding 4 mL of 0.2 M NaOH and 1 mL of 2.0 M $CaCl_2$. The concentration of p-nitrophenol released was determined spectrophotometrically at 410 nm (Shimadzu UV-1800) after filtration (Whatman ashless filter paper, grade 42) of the assay mixtures. A control without substrate was incubated under the same conditions. Enzyme activity was calculated as the difference between samples and controls, related to the samples' dry weight, and expressed as $\mu mol\ g^{-1}\ h^{-1}$.

Calculations and statistics

The amount of total as well as resin- and $NaHCO_3$-extractable P released during field exposure was calculated as difference between initial and field-exposed samples. Similarly, the release of surface P was calculated based on changes of photoelectron spectroscopy-derived P/Fe ratios between initial and field-exposed samples (Equation 1):

$$Surface\ P\ release\ (\%) = 100 \times \frac{(P/Fe)_{initial} - (P/Fe)_{exposed}}{(P/Fe)_{initial}} \quad (1)$$

The P loading of soil minerals was estimated as degree of P saturation (DPS) by Equation 2 (Pautler and Sims, 2000; Kleinman, 2017; Blombäck et al., 2021), where Fe_{AAO}, Al_{AAO}, and P_{AAO} are molar concentrations (mmol kg^{-1}) and α is an empirical sorption factor (0.5) originally developed for acidic Dutch soils to describe the sorption capacity of secondary minerals for P.

$$DPS = \frac{P_{AAO}}{\alpha(Fe_{AAO}+Al_{AAO})} \quad (2)$$

Statistical analyses were performed in SigmaPlot v. 14.5 (Systat Software, Inc.). Data were tested for normality (Shapiro-Wilk) and homogeneity of variances (Spearman rank correlation test, Brown-Forsythe). One way-analysis of variance (ANOVA) was used to test for pairwise differences between variables and differences between group means were evaluated by the Bonferroni *t*-test. To evaluate differences in P losses between study sites for each P form, data from the two depth levels were pooled to increase the number of observations. For data failing precondition tests, ANOVA on ranks was used. For variables where preconditions tests were passed, three-way ANOVA followed by Holm-Sidak tests was used to evaluate the effect of site, P form, and depth, and their interactions on P losses. Statistical significance is reported for $\alpha < 0.05$. To test for linear relationships, single and multiple linear regression models were calculated. A multiple regression model was set up to relate total P losses to specific properties of goethite samples, using stepwise forward inclusion of variables based on F statistics. In case of not normally distributed data, we used the Wilcoxon signed rank test and Spearman rank order correlations to test for differences between groups and analyze relationships among variables. Principal component analysis based on z-transformed variables was employed to reveal differences in P release patterns across sites.

Results

General soil and goethite properties

The study soils represent a gradient in P stocks as well as easily available (resin-extractable) P contents, which declined markedly from BBR over MIT to LUE (Table 1). In mineral horizons, total pedogenic Fe contents sequentially extracted by AAO and DCB (Fe_{AAO} + Fe_{DCB}) were highest at BBR, followed by MIT and LUE (Supplementary Table 1). A significant amount of Fe was bound in poorly crystalline mineral phases, as shown by moderate $Fe_{AAO}/(Fe_{AAO} + Fe_{DCB})$ ratios of 0.2–0.6. Sequential mineral extractions released substantial amounts of P ($P_{AAO} + P_{DCB}$: 1,260–2,061 mg kg^{-1} at BBR, 385–415 mg kg^{-1} at MIT, and 7–162 mg kg^{-1} at LUE), due to the intimate association of P with Fe and Al oxides. Linear regression analysis showed that total extracted P was positively related to the total extracted Fe ($r = 0.96$, $p < 0.001$). P_{AAO} was highly positively correlated with Fe_{AAO} ($r = 0.93$, $p < 0.001$, $N = 12$), but not with Al_{AAO}. In line with declining P stocks across sites, P contents in soils directly surrounding the goethite mesh bags consistently declined from BBR to LUE (Table 1). These decreases were accompanied by decreasing OC, TN, N_{min}, WEOC, and WEON values, while the WEOC/WEON ratio showed the opposite trend (Table 1).

Before field exposure, pure GOE contained no P while the total P content of GOE-OP was 1,400 ± 50 mg P kg^{-1} goethite^{-1} and those of GOE-PA 1,870 ± 10 mg P kg^{-1} goethite^{-1} ($N = 3$, mean ± SD). These values correspond to 2.2 μmol OP m^{-2} and 0.5 μmol PA m^{-2} and are close to the sorption capacities of goethite for OP and PA (Celi et al., 1999). Because of OP/PA sorption, the Zeta potential of GOE (42 ± 1 mV) decreased to −100 ± 5 mV in the goethite-P associations (see Supplementary Information for method description). For GOE-OP, 293 ± 9 and 109 ± 2 mg P kg^{-1} goethite^{-1} were sequentially extracted by an anion resin and $NaHCO_3$, respectively, resulting in 29% potentially bioavailable OP. For GOE-PA, contents of resin- and $NaHCO_3$-extractable P were 55 ± 2 and 217 ± 9 mg P kg^{-1}, respectively, which corresponds to a total of only 15% potentially bioavailable PA.

Organic carbon and nitrogen contents of exposed goethites

After field exposure for 35 months, the OC content of goethites incubated in topsoil ranged from 1.7 ± 0.4 g kg^{-1} at MIT to 4.0 ± 0.2 g kg^{-1} at LUE, while goethites exposed to subsoils had lower OC contents (Table 2). The OC accumulation by goethites, especially the P-loaded ones, showed opposite trends to soil OC

TABLE 2 Properties of pure and P-loaded (OP, orthophosphate; PA, phytic acid) goethite (GOE) exposed at two soil depths for 35 months at study sites Bad Brückenau (BBR), Mitterfels (MIT), and Lüss (LUE).

Site	P form	Depth	OC	TN	Δ OC	TP	P_{resin}	P_{bicarb}	P 2p/Fe 3s
		cm	g kg^{-1}	g kg^{-1}	g kg^{-1}	mg kg^{-1}	mg kg^{-1}	mg kg^{-1}	(x1000)
BBR	GOE	5	3.5 (0.5)	0.6 (0.1)	2.8 (0.5)	n.d.	n.d.	n.d.	0.0
BBR	GOE	30	1.6 (0.2)	0.5 (0.0)	1.0 (0.2)	n.d.	n.d.	n.d.	0.0
MIT	GOE	5	2.7 (0.7)	0.4 (0.0)	2.0 (0.7)	n.d.	n.d.	n.d.	0.0
MIT	GOE	30	1.1 (0.3)	0.5 (0.1)	0.4 (0.3)	n.d.	n.d.	n.d.	0.0
LUE	GOE	5	3.8 (1.5)	0.6 (0.1)	3.1 (1.5)	n.d.	n.d.	n.d.	0.0
LUE	GOE	30	2.9 (0.6)	0.4 (0.1)	2.2 (0.6)	n.d.	n.d.	n.d.	0.0
BBR	GOE-OP	5	2.2 (0.2)	0.6 (0.1)	1.8 (0.2)	960.0 (43.2)	56.7 (12.2)	58.5 (9.3)	36.5 (2.5)
BBR	GOE-OP	30	0.9 (0.2)	0.4 (0.1)	0.5 (0.2)	950.0 (81.6)	78.0 (5.3)	65.6 (1.0)	41.4 (3.3)
MIT	GOE-OP	5	2.1 (0.5)	0.4 (0.1)	1.7 (0.5)	980.0 (149.9)	72.7 (35.0)	67.1 (21.1)	34.9 (7.1)
MIT	GOE-OP	30	1.0 (0.2)	0.5 (0.1)	0.6 (0.2)	906.7 (70.4)	80.9 (20.8)	72.1 (9.6)	36.8 (5.9)
LUE	GOE-OP	5	4.0 (0.2)	0.6 (0.1)	3.6 (0.2)	730.0 (249.1)	16.5 (20.4)	27.0 (20.4)	24.9 (11.7)
LUE	GOE-OP	30	1.6 (0.1)	0.4 (0.1)	1.2 (0.1)	593.3 (143.8)	35.5 (23.3)	60.0 (13.6)	34.4 (4.2)
BBR	GOE-PA	5	1.9 (0.1)	0.4 (0.0)	0.8 (0.1)	1855 (125)	15.8 (2.6)	90.2 (10.9)	87.0 (3.5)
BBR	GOE-PA	30	1.2 (0.1)	0.4 (0.1)	0.0 (0.1)	1840 (29)	24.5 (2.8)	150.1 (18.7)	79.2 (5.3)
MIT	GOE-PA	5	1.7 (0.4)	0.4 (0.0)	0.5 (0.4)	1747 (54)	26.8 (5.5)	117.9 (27.6)	79.5 (9.5)
MIT	GOE-PA	30	1.1 (0.0)	0.5 (0.0)	0.0 (0.0)	1763 (21)	28.5 (6.7)	135.9 (26.0)	81.9 (5.8)
LUE	GOE-PA	5	3.5 (0.8)	0.6 (0.1)	2.4 (0.8)	1637 (155)	13.2 (3.4)	120.7 (46.1)	73.9 (12.4)
LUE	GOE-PA	30	2.2 (0.6)	0.4 (0.1)	1.0 (0.6)	1607 (103)	23.9 (12.2)	141.5 (24.6)	80.2 (6.9)

Site	P form	Depth	GalN	GlcN	MurA	Total AS	F/B	*phoD* copies	*gcd* copies
		cm	μmol g^{-1}	μmol g^{-1}	μmol g^{-1}	μmol g^{-1}	(–)	g^{-1}	g^{-1}
BBR	GOE	5	73.6 (6.6)	96.4 (19.2)	2.9 (0.0)	172.0 (26.1)	5.0 (0.9)	8.E+06 (5.E+06)	6.3E+07 (8.9E+07)
BBR	GOE	30	62.4 (6.9)	76.0 (5.8)	1.9 (0.4)	139.7 (11.4)	5.6 (0.9)	1.E+07 (2.E+06)	2.6E+06 (2.8E+06)
MIT	GOE	5	34.2 (31.1)	59.1 (21.1)	0.9 (0.0)	93.6 (51.5)	14.3 (0.0)	8.E+06 (7.E+05)	1.3E+06 (5.9E+04)
MIT	GOE	30	27.1 (22.9)	61.3 (21.0)	2.5 (0.0)	89.2 (44.7)	5.0 (0.0)	8.E+06 (1.E+06)	1.2E+06 (2.4E+05)
LUE	GOE	5	53.8 (23.6)	102.2 (32.2)	1.4 (0.0)	156.5 (47.2)	14.5 (0.0)	9.E+06 (7.E+05)	9.9E+05 (1.0E+06)
LUE	GOE	30	42.7 (20.1)	50.0 (11.1)	n.d.	92.7 (30.1)	–	9.E+06 (1.E+06)	7.7E+06 (8.7E+06)
BBR	GOE-OP	5	86.1 (7.0)	119.0 (13.7)	48.6 (62.7)	253.7 (82.7)	2.4 (1.6)	1.E+07 (4.E+06)	8.5E+06 (4.4E+06)
BBR	GOE-OP	30	51.4 (12.6)	64.9 (14.9)	2.6 (0.5)	118.9 (27.9)	3.4 (0.3)	8.E+06 (1.E+06)	1.1E+06 (1.3E+06)
MIT	GOE-OP	5	30.5 (27.5)	65.5 (10.0)	0.5 (0.5)	96.5 (37.6)	30.3 (20.7)	8.E+06 (7.E+05)	4.2E+06 (3.2E+06)
MIT	GOE-OP	30	55.2 (37.7)	79.5 (28.3)	1.4 (1.0)	136.1 (66.7)	6.7 (1.6)	8.E+06 (4.E+05)	6.3E+05 (2.2E+05)
LUE	GOE-OP	5	58.1 (38.5)	176.3 (93.1)	0.5 (0.6)	234.9 (130.3)	44.6 (28.3)	8.E+06 (3.E+06)	8.2E+06 (5.4E+06)
LUE	GOE-OP	30	44.2 (20.4)	78.0 (20.2)	n.d.	107.5 (46.7)	–	9.E+06 (8.E+05)	1.1E+06 (1.0E+06)
BBR	GOE-PA	5	n.d.	n.d.	n.d.	n.d.	–	1.E+07 (4.E+06)	2.7E+06 (7.9E+05)
BBR	GOE-PA	30	36.7 (28.0)	26.0 (36.7)	n.d.	62.7 (61.3)	–	1.E+07 (5.E+04)	7.3E+06 (5.1E+06)
MIT	GOE-PA	5	25.2 (19.0)	66.2 (28.4)	0.9 (1.3)	92.3 (48.5)	5.4 (0.0)	9.E+06 (2.E+06)	1.3E+06 (5.8E+05)
MIT	GOE-PA	30	52.6 (28.9)	82.0 (7.1)	1.1 (1.0)	135.7 (36.2)	11.6 (6.9)	9.E+06 (2.E+06)	4.2E+05 (3.4E+05)
LUE	GOE-PA	5	50.8 (32.3)	102.5 (45.3)	n.d.	153.4 (77.1)	–	1.E+07 (9.E+06)	7.9E+06 (8.9E+06)
LUE	GOE-PA	30	40.3 (20.7)	70.0 (3.6)	n.d.	96.9 (23.8)	–	9.E+06 (3.E+06)	4.9E+06 (3.8E+06)

Values in parentheses refer to standard deviation. OC, organic carbon; TN, total nitrogen; ΔOC, increase in OC upon field exposure; TP, total phosphorus; P_{resin} and P_{bicarb}, phosphorus sequentially extracted by resin and bicarbonate; P 2p/Fe 3s, phosphorus-to-iron ratio determined by X-ray photoelectron spectroscopy; GalN, GlcN, and MurA, galactosamine, glucosamine, and muramic acid; AS, amino sugars; F/B, fungal-to-bacterial C ratio; n.d., not detected; –, no data available.

contents (Figures 2a, b). The highest net uptake of OC (ΔOC) was observed at the P-poor LUE site, where the soil OC content was lowest (Table 1). For all goethite samples, ΔOC was neither linearly related to the OC content of surrounding soil nor to WEOC and WEON, or the WEOC/WEON ratio. Instead, a moderate Spearman correlation was observed between ΔOC and the F/B

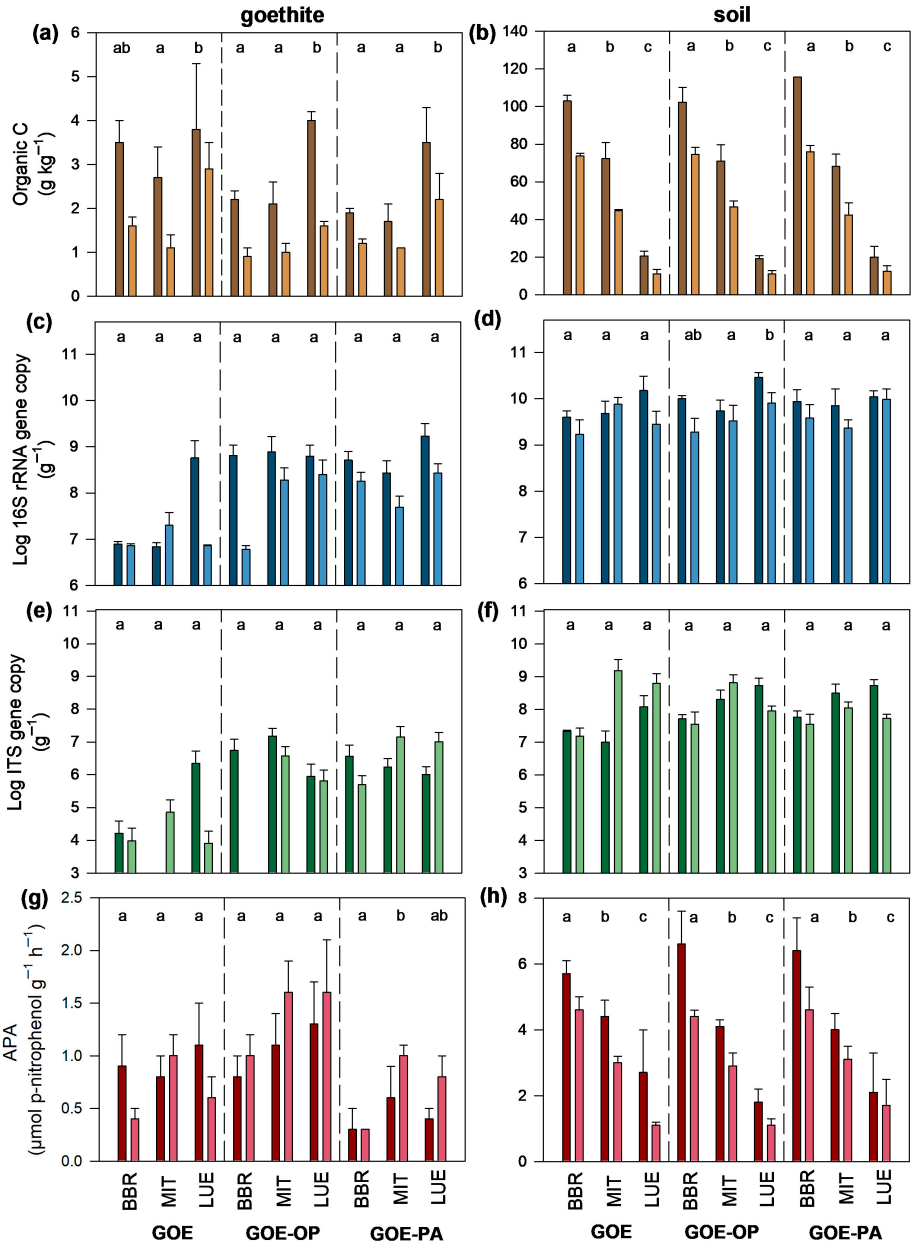

FIGURE 2
(a–h) Organic carbon contents, phylogenetic gene abundances, and potential phosphomonoesterase activity (APA) of exposed pure and P-loaded goethites and surrounding soils at the study sites Bad Brückenau (BBR), Mitterfels (MIT), and Lüss (LUE). Darker and lighter bars correspond to soil depths of 5 cm (topsoil) and 30 cm (subsoil), respectively. Goethite treatments were as follows: GOE, pure goethite; GOE-OP, goethite loaded with orthophosphate (OP); GOE-PA, goethite loaded with phytic acid (PA). The exposure time of goethites was 35 months. Different letters indicate significant differences between study sites for OP- and PA-loaded goethites pooled for both soil depths to increase the number of observations ($p < 0.05$). Error bars indicate standard deviation.

ratio of surrounding soil (all goethites: $r = 0.62$, $p < 0.001$, $N = 50$; P-loaded goethites: $r = 0.63$, $p < 0.001$, $N = 32$). Total N contents of field-exposed goethites were similar at all study sites (0.4–0.6 g kg^{-1}) (Table 2).

Amino sugars and microbial abundances in soils and exposed goethites

Total amino sugar contents were highest in soils of BBR and MIT and declined steeply toward LUE (Table 1). The content of amino sugars followed soil OC contents (Spearman $r = 0.71$, $p < 0.001$, $N = 50$), but the molar amino sugar/soil OC ratio increased in topsoils from BBR over MIT toward LUE (Table 1). Compared to the other two sites, LUE soil was characterized by significantly higher F/B ratios, exceeding those of BBR by a factor of three to four in top- and subsoil, respectively (Table 1). Bacterial 16S rRNA genes were similar in BBR and MIT topsoils, but higher in topsoil of the P-poor LUE site. In subsoils, bacterial 16S rRNA genes also increased from BBR over MIT to LUE (Figures 2c, d). Fungal ITS genes in topsoils were likewise lowest at BBR and highest at

LUE, while highest subsoil ITS copies were found in MIT due to high replicate variability (Figures 2e, f).

Following field exposure for 35 months, amino sugars could be detected in almost all goethite samples, although bacterial muramic acid was frequently below detection level. Total amino sugar contents accounted for 2%–7% of that in the corresponding soil, without consistent differences between pure and P-loaded goethites (Table 2). For 22 goethite samples, it was possible to calculate F/B ratios, which were significantly higher than those of the corresponding soil (Wilcoxon $p < 0.001$). Colonization of goethite samples by bacteria and fungi was further evidenced by phylogenetic data, with bacterial 16S rRNA genes exceeding those of fungal ITS (Figures 2c, e). Except from pure goethite exposed in LUE topsoil, bacterial and fungal genes tended to be lower for pure goethite than for P-loaded goethites (Figures 2c, e).

Phosphomonoesterase activity in soils and exposed goethites

Acid phosphomonoesterase activity of soil surrounding the mesh bags followed the soil P availability gradient: BBR > MIT > LUE. Values ranged from 1.1 ± 0.1 to 6.6 ± 1.0 μmol p-nitrophenol g^{-1} h^{-1} and were higher in topsoil than subsoil (Figure 2h). After 35 months of field exposure, acid phosphomonoesterase activity could be measured in all goethite samples, although at lower levels than in corresponding soil (Figures 2g, h). For both P forms, acid phosphomonoesterase activity was inversely related to that of surrounding soil (LUE > MIT > BBR). When considering all sites and depth levels, acid phosphomonoesterase activity was significantly higher for OP-GOE than PA-GOE ($p < 0.001$, $N = 36$).

Release of goethite-bound phosphate and phytate

In most cases, Fe/Zr weight ratios of exposed goethites (mean: 42 ± 7) were similar to those of initial goethites (mean: 40 ± 1), indicating no systematic loss of goethite particles from mesh bags during field incubation (Supplementary Table 2). This was supported by absent or only minor "orange staining" of soil underneath mesh bags upon retrieval. Both X-ray fluorescence and photoelectron analyses showed no detectable P accumulation for initially P-free goethite after 35 months, so that observed P losses from P-loaded goethites represent gross P mobilization. Total P losses ranged between 1% and 58%, with higher losses for GOE-OP than GOE-PA, irrespective of site or soil depth (Figure 3a). Three-way ANOVA indicated that total P losses significantly depend on

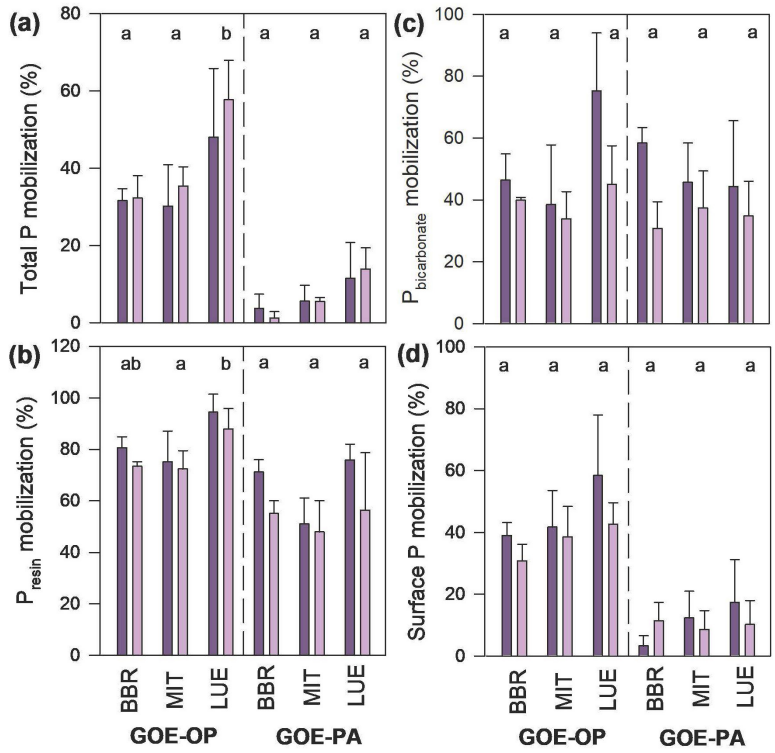

FIGURE 3
(a–d) Mobilization of orthophosphate-P and phytic acid-P bound to goethite during exposure for 35 months in soils at the study sites Bad Brückenau (BBR), Mitterfels (MIT), and Lüss (LUE). Darker and lighter bars correspond to soil depths of 5 cm (topsoil) and 30 cm (subsoil), respectively. Goethite treatments: GOE-OP, goethite loaded with orthophosphate (OP); GOE-PA, goethite loaded with phytic acid (PA). Total P mobilization was determined before and after exposure by X-ray fluorescence spectrometry, while resin- (P_{resin}) and bicarbonate-extractable P (P_{bicarb}) mobilization was determined using a sequential extraction approach. Surface P mobilization was derived from surface P/Fe ratios determined by X-ray photoelectron spectroscopy. For more methodological information, please refer to the section "Materials and Methods." Different letters indicate significant differences between study sites for OP- and PA-loaded goethites pooled for both soil depths to increase the number of observations ($p < 0.05$). Error bars indicate standard deviation.

site and P form but not on depth, with no interactions among variables (Supplementary Table 3). Total P losses followed the order: BBR < MIT < LUE, and significantly more P was released at the P-poor LUE site. As expected, highest OP and PA losses occurred in the resin-extractable P fraction (P_{resin}), with maximal values reaching 94% for GOE-OP and 71% for GOE-PA (Figure 3b). For each P form, the highest P_{resin} release was recorded for the P-poor LUE site, with significantly higher P_{resin} losses in topsoil than subsoil. Results of the 3-way ANOVA show that P_{resin} losses significantly depend on site, P form, and depth, but without interactions among variables (Supplementary Table 3). Phosphorus losses from the $NaHCO_3$-extractable P fraction ranged from 31% to 75%, with less clear differences among the two P forms, but with the general trend of higher losses in topsoil than in subsoil (Figure 3c).

Considering the sum of P_{resin} and P_{bicarb} as potentially bioavailable P, between 36% and 90% of this fraction has been released over the experimental period, again with highest losses for OP at LUE. Especially for these samples, microscope images revealed fungal hyphae colonizing the goethite, with some hyphae covered not only by goethite particles but also by bacteria (Figure 4). Principal component analysis revealed that the first two principal components accounted for 62% of the variance in P losses in combination with soil and goethite properties after 35 months of exposure (Figure 5). Loadings of soil P, OC, and TN contents on principal component 1 were inverse (−0.78, −0.81, and −0.80, respectively) to those of the OC content and ΔOC of exposed P-loaded goethites (0.76 and 0.78, respectively).

Vectors for percentage losses of P fractions suggest that P release was closely linked to OC accumulation (Figure 5). Contrary to the vector of soil phosphomonoesterase activity, the vector of phosphomonoesterase activity in exposed goethites pointed toward GOE-OP samples with their high P losses. The P-poor LUE site, which showed the highest losses of adsorbed P, clearly differed from the other sites and coincided with the soil F/B vector. Based on correlation analyses, we first tested, which soil properties explained observed P losses. For the entire data set, P_{resin} losses correlated significantly positively with the F/B ratio, bacterial 16S rRNA as well as *phoD* and *gcd* copy numbers (Figure 6). For OP, losses of total P, P_{resin}, P_{bicarb}, and total mobilizable P were positively correlated with the soil F/B ratio, whereas for PA no such relations existed (Figure 6). Phosphorus losses were negatively related to total amino sugar and muramic acid contents, again especially for OP, generally mirroring the trends in soil microbial biomass (BBR > MIT > LUE; Lang et al., 2017). For both P forms, total P losses correlated negatively with soil phosphomonoesterase activity. Overall, P form affected P release more than soil depth.

For P-loaded goethites, losses of total P, P_{resin}, P_{bicarb}, and total mobilizable P correlated positively with ΔOC. Especially in topsoil and for GOE-OP, P losses related closely to post-exposure OC contents. For goethites exposed to topsoil or subsoil, total P loss as well as total mobilizable P correlated positively with phosphomonoesterase activity (Figure 6). In a multiple regression model for the entire data set, total P loss was best predicted by ΔOC and phosphomonoesterase activity (APA): Total P loss (%) = −8.3 + 6.8 ΔOC + 25.9 APA (r = 0.80, p < 0.001, N = 35). No linear relations were observed between P loss and *phoD* and *gcd* genes (Figure 6).

Chemical surface changes of exposed goethites

We examined the chemical surface composition of goethites before and after field exposure by X-ray photoelectron spectroscopy. Surfaces of non-exposed goethites already contained considerable quantities of adventitious C (GOE and GOE-OP, 44 ± 4 at%, N = 6) and/or C inherited from adsorbed PA (GOE-PA, 45 ± 2 at%, N = 3) (Supplementary Table 4). In line with bulk OC trends, surface C contents of goethites increased over 35 months. No surface N accumulation was observed (Supplementary Table 4), probably because surface N contents were below the level of quantification. Surface P losses correlated positively with X-ray fluorescence-derived total P losses as well as ΔOC and phosphomonoesterase activity (Figure 6), and were significantly higher for OP than for PA. For both P forms, surface P loss was lowest at BBR and highest at LUE, and in almost all cases greater in topsoil than subsoil (Figure 3d). Three-way ANOVA revealed that surface P loss depended primarily on P form and was less affected by site and depth, or interactions (Supplementary Table 3).

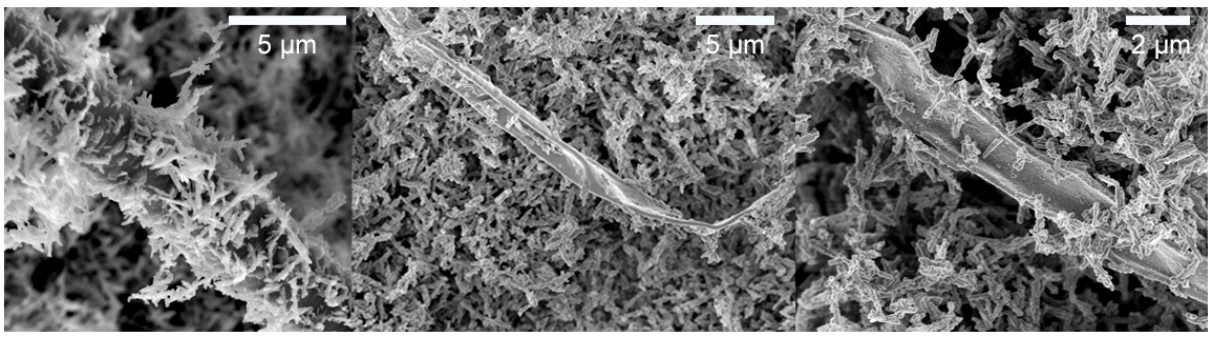

FIGURE 4
Scanning electron microscopy images showing partially desiccated hyphae growing through P-loaded goethite after exposure for 35 months in the P-poor soil at Lüss. Note the intimate attachment of goethite crystals and bacterial cells at the hyphae surface in the left image.

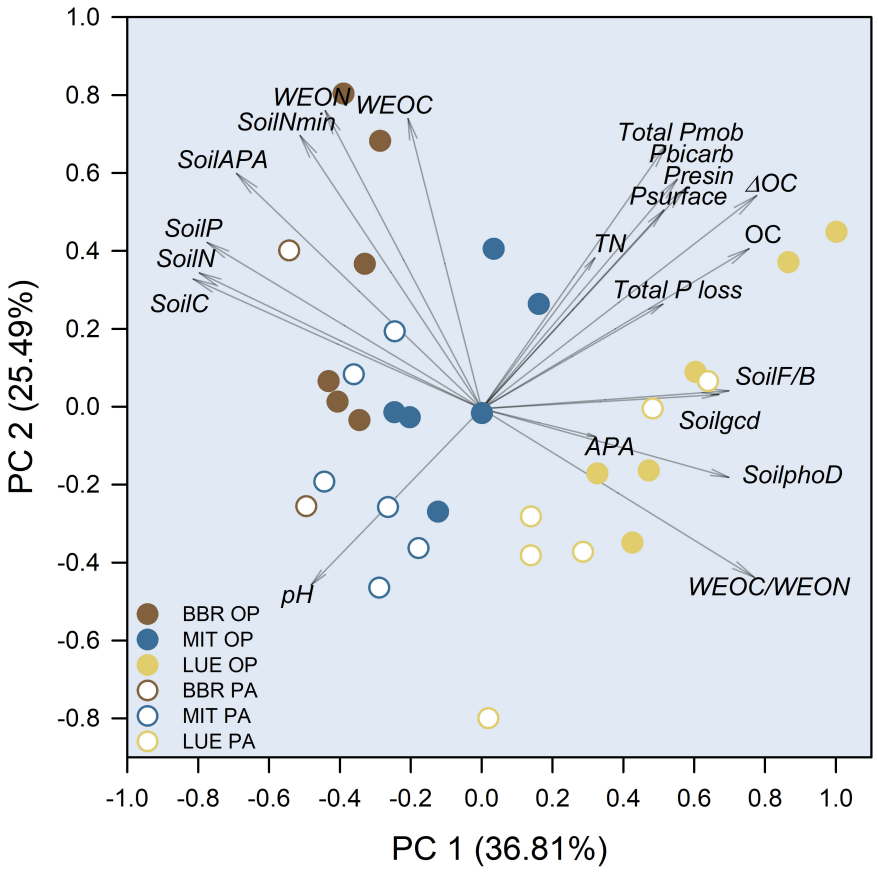

FIGURE 5
Principal component plot of variables in relation to the observed P mobilization from goethite loaded with orthophosphate (OP) and phytic acid (PA) during exposure for 35 months in soils at the study sites Bad Brückenau (BBR), Mitterfels (MIT), and Lüss (LUE). SoilC, SoilN, and SoilP, total organic carbon, nitrogen, and phosphorus contents of soils; SoilNmin, inorganic nitrogen content of soils; WEOC and WEON, water-extractable organic carbon and nitrogen of soils; SoilF/B, fungal-to-bacterial C ratio of soils; Soilgcd and SoilphoD; *gcd* and *phoD* gene copies of soils; SoilAPA and APA, acid phosphomonoesterase activity of soils and goethites after field exposure; OC, TN, and ΔOC, organic carbon and total nitrogen content and increase of organic carbon in goethites after field exposure; Total P loss, percentage release of total phosphorus; Presin and Pbicarb, percentage release of resin- and bicarbonate-extractable phosphorus; Total Pmob, percentage release of resin- plus bicarbonate-extractable phosphorus; Psurface, percentage release of surface-bound phosphorus.

Discussion

Microbial colonization of goethite in soils of different P status

Mesh bags filled with GOE, GOE-OP, and GOE-PA have been exposed to a steep soil P availability gradient for 35 months in topsoils (5 cm) and subsoils (30 cm), with LUE considered a P-limited site based on fertilization experiments (Zavišiæ et al., 2018). All goethites, especially GOE and GOE-OP, provided initially C-poor habitats, thus simulating fresh mineral surfaces produced by mineral weathering. The observed OC accumulation on goethites (ΔOC; max. 0.2 mg m^{-2}) at all sites was similar to those recently observed for goethite and illite (clay mineral) exposed for 60 months to soils of forest and grassland ecosystems across Germany (Bramble et al., 2024). The higher ΔOC at LUE might have been caused by the sandier soil texture, which supports water and DOM transport and thus allows for microbial colonization of goethite surfaces. The provision of C substrates might have contributed to higher P losses at LUE, as the microbially mediated release of mineral-bound P has been shown to depend on C availability (Brucker et al., 2020). Particularly at LUE with high goethite ΔOC values, water-extractable soil OM had a wider OC/ON ratio (Table 1), suggesting more DOM compounds with a higher sorption affinity than at the other two sites. Contribution of DOM sorption to the observed OC accumulation on goethite surfaces is reasonable at acidic soil pH, which promotes sorptive interactions of goethite with DOM. However, unlike pure GOE, GOE-OP and GOE-PA had a negative surface charge, implying less efficient sorptive interactions with negatively charged DOM. Consequently, surface OC accumulation was presumably more related to microbial colonization than to DOM adsorption.

Noteworthy, ΔOC showed an opposite trend to soil OC and was positively correlated with the soil F/B ratio. This suggests a faster OC accumulation by exploring fungal communities in LUE soil. We also observed that goethites analyzed for F/B ratios showed higher values than corresponding soils (Tables 1, 2). Recolonization experiments with in-growth tubes exposed for 18 months at the study sites (0-20 cm) demonstrated a strong contribution of ectomycorrhizal fungi, especially at P-poor LUE and MIT, but not BBR (Müller et al., 2020). Brandt et al.

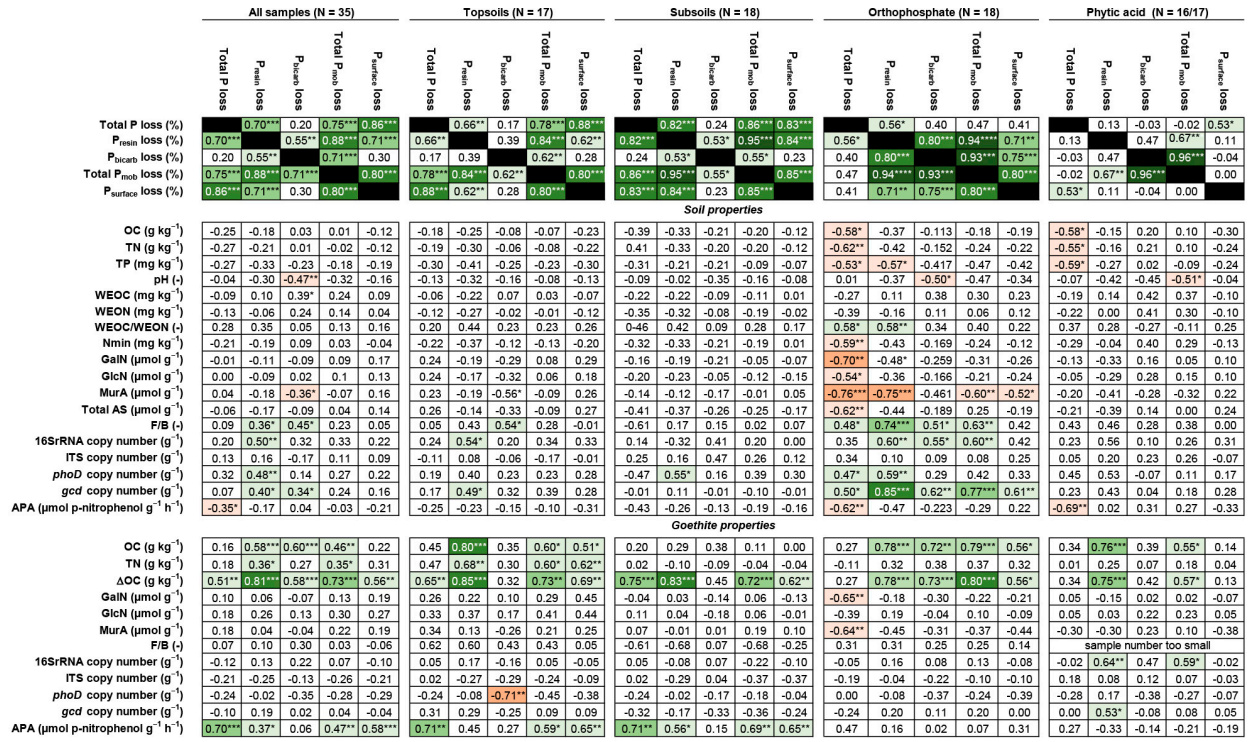

FIGURE 6

Spearman rank order correlations between different forms of P loss (upper panels) as well as between P losses and the properties of soil (intermediate panels) and goethites (lower panels). P_{resin} and P_{bicarb}, resin- and bicarbonate-extractable phosphorus; Total P_{mob}, sum of resin- and bicarbonate-extractable phosphorus; $P_{surface}$, release of surface-bound phosphorus; OC, TN, and TP, total organic carbon, nitrogen, and phosphorus; ΔOC, organic carbon increase in goethites; WEOC and WEON, water-extractable organic carbon and nitrogen; Nmin, inorganic nitrogen; GalN, GlcN, and MurA, galactosamine, glucosamine, and muramic acid; AS, amino sugars; F/B, fungal-to-bacterial C ratio; APA, acid phosphomonoesterase activity. Significant positive and negative correlations are colored green and red, respectively, for better visibility (*$p < 0.05$; **$p < 0.01$; ***$p < 0.001$).

(2024) also reported the preferential colonization of juvenile goethite and illite surfaces by fungi, resulting in higher F/B ratios compared to surrounding soil. Microbial OC accumulation is also suggested by higher phylogenetic gene abundancies in P-loaded goethites compared to pure GOE ($p < 0.05$; n.s. only for the difference between GOE and GOE-OP for fungal ITS), hinting at a directional exploration of goethites for P, as shown in other mesh-bag studies (e.g., Rosenstock et al., 2016). In short, our data indicate that the OC increase on exposed goethites was tightly linked to microbial colonization, particularly by fungi.

Phosphorus release depends on P form

Our study shows that both P forms adsorbed to goethite were released when exposed to top- and subsoil of old-grown beech forests for 35 months, even at low soil pH. Therefore, our first hypothesis that both adsorbed P forms can be mobilized regardless of the P status of soils cannot be refuted. The same is true for our second hypothesis stating that OP is generally more mobilizable than PA. The release of P was studied by X-ray fluorescence spectrometry and photoelectron spectroscopy, showing similar patterns for both P forms across the soil P gradient. The observed percentage release of OP (30%–58%, 423–810 mg kg^{-1} $goethite^{-1}$) was similar to those observed for goethite-OP-sand samples exposed for 13 months in less acidic (pH 5.6-7.6), serpentine-rich soils under ectomycorrhizal vegetation in the Italian Alps (D'Amico et al., 2020). These authors also observed a larger release of OP (up to 65%) than PA (up to 45%).

Preferential release and subsequent plant utilization of OP over phytate-P has also been documented in few laboratory studies (Martin et al., 2004; Andrino et al., 2019; Amadou et al., 2022). Amadou et al. (2022) showed in a 15-days greenhouse experiment that more P derived from goethite-bound OP than from bound PA (21 vs. 1%) was taken up by ryegrass. The lower uptake of PA has been explained by the fact that organic P requires enzymatic hydrolysis beforehand (Andrino et al., 2019) and that the phytase activity was low (Martin et al., 2004). In fact, enzymatic hydrolysis of PA appears only possible after PA desorption from mineral surfaces (Giaveno et al., 2010). While OP is bound to goethite by either mono- or binuclear innersphere complexes, PA can form more than two P-O-Fe bonds at Fe oxide surfaces (Chen and Arai, 2019). Even though the exclusive presence of outersphere complexes of PA on goethite surfaces at pH 2–12 has been suggested (Johnson et al., 2012), the experimental and modeling approach of Ganta et al. (2021) indicted that PA forms up to three innersphere bonds with surface-Fe under acidic conditions. Such multiple attachments reduce the likelihood of PA desorption and exchange with organic ligands, which accords with lower amounts of resin-extractable P for PA- than OP-loaded goethites (55 vs. 293 mg

kg^{-1}; 3 vs. 21% of total P). Notably, P losses over 35 months never exceeded the "mobilizable" P fraction determined by sequential extraction with resin and $NaHCO_3$. With 89%, this fraction was highest in P-poor LUE topsoil. Assuming that the exposure time over 35 months was long enough for the release of mobilizable P, the remaining P was supposedly more strongly bound, for example, via stronger electrostatic attractions (Krumina et al., 2016). Our findings harmonize the observations, that, although a significant fraction of adsorbed P can be mobilized, an even larger fraction of oxide-bound P is not readily mobilizable and thus bioavailable. The preferential mobilization of adsorbed OP in comparison to PA observed in field and laboratory plant-growth studies might also explain the relative enrichment of organic P with increasing soil development (Lang et al., 2017). This has implications for plant nutrition, as P limitation in old, weathered soils can be caused not only by sink- or depletion-driven processes (Vitousek et al., 2010), but also by shifts toward less bioavailable organic P forms. Our study confirms that P form and thus binding strength control the extent of P release into solution, which is prerequisite for biological P uptake following hydrolytic dephosphorylation in case of organic P.

Abiotic and biotic processes are both involved in P release

Potential mechanisms for the release of P from Fe oxides under oxic conditions include (i) desorption of P compounds driven by P concentration gradients, (ii) proton- or ligand-promoted mineral dissolution, and (iii) exchange with organic compounds, including microbial metabolites and root exudates. Our data suggest that both desorption and active microbial mining are involved in the mobilization of adsorbed P. Since the goethite-P associations have been produced under similar pH conditions as the study soils, P release during field exposure was likely not caused by pH effects. D'Amico et al. (2020) suggested that losses of adsorbed P in only slightly acidic to alkaline soils of the Italian Alps were tightly coupled to the dissolution of goethite. Our X-ray photoelectron spectroscopy data showed that surface P/Fe ratios declined markedly, especially for OP at LUE (Table 2). Declining P/Fe ratios suggest that adsorbed P was removed without goethite dissolution and/or that P was faster released from goethite than reductively dissolved Fe. As the reductive and proton-promoted dissolution of goethite can be assumed to be minor in our field experiment, our data imply the desorption of adsorbed P and its exchange with organic ligands produced by microorganisms.

Our goethite samples were initially saturated with OP and PA, and the resin-extractable P fraction of GOE-OP and GOE-PA accounted for 21 and 3% of total P, respectively, which is similar to values reported by Martin et al. (2004). Given that P desorption increases with the degree of P surface saturation (Parfitt, 1979), exposing highly P-loaded goethites to low-P soil solutions results in P desorption upon re-equilibration. Because goethite-colonizing microorganisms also facilitate the formation of P concentration gradients by the uptake of dissolved P, we infer that desorption of P into P-undersaturated soil solutions is a very plausible scenario. Based on adsorption isotherms (Celi et al., 1999), P solution concentrations lower than 2 μM are expected to induce considerable desorption of both P forms. In solutions leached from topsoil horizons at LUE, total P concentrations measured in 2018/19 frequently fell below this limit, which was less often the case for BBR topsoil (Fetzer and Hagedorn, 2021).

We also found indications of other P-release mechanisms connected to microbial P mining. As consequence of initial P desorption from goethite, subsequent P release will tremendously slow down. This phenomenon is ascribed to the decreasing repulsion between adsorbed P molecules and the increasing positive surface charge of goethite upon P desorption (Krumina et al., 2016). Declining desorption of OP and PA from goethite in different media (H_2O, KCl, oxalate) with decreasing surface P loading has also been documented by Yan et al. (2015). Lower surface P loadings also decreased the effectiveness of the saprotrophic P-solubilizing fungus *Mortierella* sp. to release P bound to silicate clays and goethite (Osorio and Habte, 2013) and the arbuscular mycorrhizal fungus *Glomus tenuis* to mobilize P from goethite (Parfitt, 1979). Consequently, the degree of surface P saturation likely defines the magnitude of abiotic and biotic P mobilization.

In addition to the easily released P_{resin}, we found that the more strongly bound bicarbonate-extractable P was also significantly reduced, suggesting an active release by microorganisms via the production of P-mobilizing organic compounds. The release of P_{bicarb} was highest at the P-deficient LUE site, which coincides with the highest soil F/B ratio and largest OC accumulation in goethite samples. Furthermore, *gcd* gene numbers, encoding for glucose dehydrogenase and representing the potential for the bacterial production of P-solubilizing organic acids, were highest in LUE soil (Table 1). The observed positive correlation between P loss and soil *gcd* genes (Figure 6) suggests that bacteria also contribute to the release of oxide-bound P. A higher microbial activity directed toward P acquisition under increasing soil P scarcity was also indicated by a higher phosphomonoesterase activity for GOE-OP and GOE-PA at the P-poor sites as well as by a positive correlation between phosphomonoesterase activity measured in goethite samples and total P loss. All these observations support our hypothesis that in P-limited recycling ecosystems like LUE, more adsorbed P can be mobilized by adapted microbial communities than at sites with higher P availability. This P-mobilizing capability seems to be more effective for the exploitation of oxide-bound OP, while the higher binding strength of PA in comparison to OP generally impairs PA desorption. The latter likely explains why phytase genes were generally low in topsoils of our study soils (Bergkemper et al., 2016). We also observed a significant contribution of alkaline phosphatase genes (*phoD*) in soils and all goethite samples, while genes coding for acid phosphatase were below detection levels. The abundance of *phoD* in goethite samples suggests that especially microbes colonizing the goethite carry the genetic potential for the production of alkaline phosphatase, although its actual expression remains unclear.

Oxide-bound phosphorus: a quantitatively relevant nutrient source?

Sorption of P to Fe and Al oxides can induce severe soil P limitation (Vitousek et al., 2010; Santoro et al., 2024). On the other hand, reports about effective exploitation of adsorbed P by microbe-plant associations, even within relatively short

time (Merlin et al., 2016; Andrino et al., 2019; D'Amico et al., 2020; Pastore et al., 2020; Amadou et al., 2022), warrant the harmonization of this apparent contradiction. As mentioned earlier, P loadings of minerals in most field and laboratory experiments are very high (≥70% saturation) due to experimental necessities (Andrino et al., 2019; D'Amico et al., 2020; Amadou et al., 2022; Almeida et al., 2024). Phosphorus desorption upon re-equilibration in the absence of abundant free adsorption sites will thus certainly overestimate P losses and biological P use compared to natural conditions. Furthermore, P compounds in soil might be more heterogeneously distributed than in mesh bags or plant pots/compartments (Werner et al., 2017; Rodionov et al., 2020) and located in small intra- and interparticle pores of minerals (Mikutta et al., 2006), potentially limiting the spatial accessibility of adsorbed P compounds.

To address the question how quantitatively important mineral-bound P is for forest nutrition at our study sites, we first estimated the stocks of P adsorbed to secondary (Fe and Al) minerals. We relied on AAO-extractable P, which predominantly represents P adsorbed to poorly crystalline minerals that harbor most adsorbed P (except at BBR; Supplementary Table 1). The P_{AAO} stocks of the first 30 cm of mineral soil accounted for 116 g m^{-2} at BBR, 67 g m^{-2} at MIT, and 9 g m^{-2} at LUE. Based on the P_{AAO} stocks, we applied our observed *in-situ* P release rates for OP and PA, scaled to 12 months, ignoring that P release is likely non-linear and dependent on seasons. To account for the dependence between the P loading of minerals and extent of P release (Yan et al., 2015), the derived stocks of "potentially mobilizable adsorbed P" were multiplied with the respective DPS values (Equation 2). The results show that the stocks of potentially mobilizable adsorbed P in the uppermost 30 cm vary tremendously depending on P form: In case all adsorbed P in the soils was OP, potentially mobilizable P would amount to 15 kg ha^{-1} a^{-1} at BBR and 1.9 kg ha^{-1} a^{-1} at LUE. If all adsorbed P was PA, the mobilizable adsorbed P would only amount to 1.6 kg ha^{-1} a^{-1} at BBR and 0.5 kg ha^{-1} a^{-1} at LUE. Although our study was limited to only two P forms, the study by Amadou et al. (2022) suggests that the plant-use of other adsorbed organic P forms like glucose-6-phosphate or glycerophosphate, when bound to clay minerals and Al hydroxide, was in a similar range. As topsoils of BBR and MIT contained high shares of organic P on mineral surfaces (>50%) (Stahr et al., 2018), the potentially mobilizable adsorbed P might be in between or, more likely, at the lower end of values reported above (Supplementary Table 5).

Despite the uncertainty of our approach and the restriction to the uppermost mineral soil, we can compare these estimates with the annual P uptake by forest vegetation. This is because in mineral soils of temperate beech forests, the main portion of fine roots relevant for P uptake usually resides in the upper soil (top ~ 30–40 cm) (Leuschner et al., 2001; Meier and Leuschner, 2008). The P demand of beech forests can be approximated with 9 kg ha^{-1} a^{-1}, based on a gross primary productivity of 12.6 Mg ha^{-1} a^{-1} and bulk tree P content at MIT of 0.71 g kg^{-1} (Uhlig and von Blanckenburg, 2019). This value closely matches the P uptake of 9.6 kg ha^{-1} a^{-1} reported for a 70-years old hardwood forest dominated by beech, maple, and birch, of which about 3.6 kg ha^{-1} derived from the mineral soil (Yanai, 1992). The estimated amount of mobilizable adsorbed P at the sandy LUE site within the uppermost 30 cm of less than about 0.5 kg ha^{-1} a^{-1} suggests that mineral-bound P, although being most vulnerable to mobilization, could likely not suffice forest P demands, simply because of the limited abundance of reactive minerals and their low P loadings.

Although many studies use an α value of 0.5 to calculate the DPS of soils (Equation 2; Blombäck et al., 2021), it must be emphasized that this value is not strictly experimentally justified. Higher values of 0.68 have been suggested, representing a higher P sorption capacity of soils when accounting also for slow P sorption processes (Pautler and Sims, 2000). Applying an α value of 0.68 to our soils further reduced the amount of potentially mobilizable P by ~30%, meaning that less than about 0.3 kg P ha^{-1} a^{-1} would be mobilizable at the LUE site. This estimate can well explain why plant P acquisition at this P-poor site is more depending on P recycling in the forest floor layer (Lang et al., 2017). For comparison, at the P-poor LUE site, leaf litterfall P amounts to 1.6 kg ha^{-1} a^{-1} and mineralizable P in the forest floor layer to about 8 kg ha^{-1} a^{-1} (Brödlin et al., 2019). These values clearly exceed the estimated stock of potentially mobilizable mineral-bound P. While more P is recycled by litterfall (2.3 kg ha^{-1} a^{-1}) at BBR, slightly less P is provided by mineralization in the forest floor layer (~ 2 kg ha^{-1} a^{-1}) (Brödlin et al., 2019). Consequently, the stocks of potentially mobilizable mineral-bound P at MIT and BBR (α = 0.5: ~1.0–1.6 kg ha^{-1} a^{-1}; α = 0.68: ~0.7-1.2 kg ha^{-1} a^{-1}) in the top 30 cm of mineral soil are similar to the P mineralization in forest floor layers. This finding suggests that P, especially OP, when bound to secondary minerals in topsoils, can be a quantitatively relevant P pool for forest nutrition, potentially supplemented by P bound in deeper soil (Göransson et al., 2006).

Although our approach comes with uncertainties and considers only the uppermost soil, estimates of potentially mobilizable adsorbed P for BBR and MIT clearly show that mineral-bound P partly re-enters the biological cycle within relatively short time. Nevertheless, the quantitative role of subsoil P for plant nutrition still deserves attention. In a previous mesocosm experiment, we showed that goethite-adsorbed P incorporated into a subsoil from LUE, even at a high surface P saturation level, was insufficient to support beech growth (Klotzbücher et al., 2020). On the one hand, this finding could be explained by the young saplings used, which probably had not yet developed a diverse and efficient symbiotic network compared to an old-grown forest (Twieg et al., 2007). On the other hand, the low P loading of secondary minerals in this subsoil (Bw horizon, 35–100 cm depth) might have resulted in the re-sorption of P desorbed from the P-saturated goethite (Klotzbücher et al., 2020). Given the generally lower P contents and P loadings of secondary minerals, and lower fine root and microbial biomass contents in subsoil than in topsoil, the contribution of adsorbed P in subsoils to plant nutrition is probably limited. This conclusion is supported by the lower P_{resin} release from goethites when exposed to subsoils compared to topsoils. Noteworthy, at our study sites we did not observe P immobilization by pure GOE during 35 months, suggesting that a large part of P leaving the forest floor is not even entering the deeper soil.

Taking all presented evidence together, our third hypothesis that P mobilization occurs at rates quantitatively relevant for plant nutrition can only be partly confirmed. Our data emphasize that P adsorbed to secondary minerals can at least significantly contribute to forest P nutrition in more P-rich soils, especially when OP accumulates on mineral surfaces and inputs of P and C are sufficient to promote active P-mining microbial communities.

In context of the "open vs. tight P cycle" framework proposed in the German priority program SPP 1685 "Ecosystem Nutrition: Forest strategies for limited phosphorus resources" (Lang et al., 2017), our DPS-scaled estimates and microbial signatures consolidate a gradient-level picture in which Fe-oxide-bound OP supplements plant P supply at the P-richer BBR and MIT sites, while forest floor recycling dominates at the P-poor LUE site. In the Supplementary Table 6, we provide a summary of the supporting and contrasting results from SPP 1685, broken down by site and process, to show how our experimental results comply with the consortium's broader findings on P recycling.

Conclusion

Examining the fate of P compounds after sorptive immobilization by secondary minerals is important for understanding soil P cycling and the contribution of mineral-bound P to forest nutrition. This study explored the *in-situ* release of goethite-bound OP and PA over 35 months in acidic temperate forest soils along a soil P availability gradient. Higher losses by abiotic desorption and active microbial mining were observed for OP, in line with the higher stability of adsorbed PA. The fact that P losses from P-saturated goethite never exceeded the mobile P fraction (resin- plus $NaHCO_3$-extractable P) suggests that a high P surface saturation of mineral surfaces promotes the (a)biotic mobilization of adsorbed P. In the same line, a low abundance of free sorption sites causes weaker surface complexes, thus facilitating biological P utilization. Our findings confirm the dual role of Fe oxides as sink and source of bioavailable P. Although we found indications of a more efficient microbial community under P-deficient conditions, our tentative assessment on the contribution of adsorbed P to forest nutrition suggests that this community was unable to outweigh the P demand of forests owing to low P contents of the sandy parent material. This finding aligns with the concept of P-poor "recycling systems," where the P demand of forests depends more on organic P in forest floor layers than on P in mineral soil, thus stressing the relevance of organic soil layers for forest nutrition at sandy P-poor sites. Conversely, at loamy P-rich sites, the higher stocks of potentially mobilizable adsorbed P, especially OP, indicate a possible role of adsorbed P in forest nutrition. Finally, our study emphasizes that high surface P saturation levels of minerals commonly used in greenhouse and field experiments likely lead to an overestimation of natural plant P acquisition, calling for experimental setups that trace P fluxes from mineral surfaces into plants under more realistic conditions.

Data availability statement

The original contributions presented in the study are publicly available. This data can be found here: https://sadar.uni-halle.de//handle/1914118/21; http://dx.doi.org/10.25673/1914118-13.

Author contributions

RM: Conceptualization, Formal analysis, Funding acquisition, Investigation, Supervision, Writing – original draft. CM: Formal analysis, Writing – original draft, Visualization. JB: Conceptualization, Supervision, Writing – review & editing. DD: Investigation, Writing – review & editing. GD: Investigation, Writing – review & editing. GG: Conceptualization, Supervision, Writing – review & editing, Funding acquisition. RJ: Investigation, Writing – review & editing. AC: Investigation, Writing – review & editing. SS: Investigation, Writing – review & editing. MS: Investigation, Writing – review & editing. EV: Investigation, Writing – review & editing. AA: Conceptualization, Investigation, Writing – review & editing, Formal analysis.

Funding

The author(s) declared that financial support was received for this work and/or its publication. The study was carried out in the framework of the priority program 1685 "Ecosystem Nutrition: Forest strategies for limited phosphorus resources" funded by the German Research Foundation (Project number: 240950800). The X-ray photoelectron spectrometer, X-ray fluorescence spectrometer, and scanning electron microscope were funded by the German Research Foundation (Grants: 319810681, 427255914, and 457729156, respectively).

Acknowledgments

We acknowledge Anika Klotzbücher, Suanne Ulrich, and Klaus Kaiser for their support in planning and conducting the field campaign. We are further thankful to Alexandra Boritzki, Christine Krenkewitz, and Tobias Schön for their assistance in the laboratory, Rüdiger Kilian for support with scanning electron microscopy, and Leopold Sauheitl and Michael Schloter for discussion and advice.

Conflict of interest

The author(s) declared that this work was conducted in the absence of any commercial or financial relationships that could be construed as a potential conflict of interest.

The authors SS, MS, and EV declared that they were an editorial board member of Frontiers, at the time of submission. This had no impact on the peer review process and the final decision.

Generative AI statement

The author(s) declared that generative AI was not used in the creation of this manuscript.

Any alternative text (alt text) provided alongside figures in this article has been generated by Frontiers with the support of

artificial intelligence and reasonable efforts have been made to ensure accuracy, including review by the authors wherever possible. If you identify any issues, please contact us.

Publisher's note

All claims expressed in this article are solely those of the authors and do not necessarily represent those of their affiliated organizations, or those of the publisher, the editors and the reviewers. Any product that may be evaluated in this article, or claim that may be made by its manufacturer, is not guaranteed or endorsed by the publisher.

Supplementary material

The Supplementary Material for this article can be found online at: https://www.frontiersin.org/articles/10.3389/ffgc.2026.1783866/full#supplementary-material

References

Almeida, J. P., Roobroeck, D., Mårtensson, L.-M. D., Rosero, P., Kimutai, G., Kätterer, T., et al. (2024). Desorption of mineral-bound phosphorus across different cropping systems and agronomic strategies to promote efficient input use. *Appl. Soil Ecol.* 203:105672. doi: 10.1016/j.apsoil.2024.105672

Amadou, I., Faucon, M.-P., and Houben, D. (2022). Role of soil minerals on organic phosphorus availability and phosphorus uptake by plants. *Geoderma* 428:116125. doi: 10.1016/j.geoderma.2022.116125

Andrino, A., Boy, J., Mikutta, R., Sauheitl, L., and Guggenberger, G. (2019). Carbon investment required for the mobilization of inorganic and organic phosphorus bound to goethite by an arbuscular mycorrhiza (*Solanum lycopersicum* x *Rhizophagus irregularis*). *Front. Environ. Sci.* 7:26. doi: 10.3389/fenvs.2019.00026

Andrino, A., Guggenberger, G., Kernchen, S., Mikutta, R., Sauheitl, L., and Boy, J. (2021). Production of organic acids by arbuscular mycorrhizal fungi and their contribution in the mobilization of phosphorus bound to iron oxides. *Front. Plant Sci.* 12:661842. doi: 10.3389/fpls.2021.661842

Appuhn, A., and Joergensen, R. (2006). Microbial colonisation of roots as a function of plant species. *Soil Biol. Biochem.* 38, 1040–1051. doi: 10.1016/j.soilbio.2005.09.002

Appuhn, A., Joergensen, R. G., Raubuch, M., Scheller, E., and Wilke, B. (2004). The automated determination of glucosamine, galactosamine, muramic acid, and mannosamine in soil and root hydrolysates by HPLC. *J. Plant Nutr. Soil Sci.* 167, 17–21. doi: 10.1002/jpln.200321302

Bach, H.-J., Tomanova, J., Schloter, M., and Munch, J. C. (2002). Enumeration of total bacteria and bacteria with genes for proteolytic activity in pure cultures and in environmental samples by quantitative PCR mediated amplification. *J. Microbiol. Methods* 49, 235–245. doi: 10.1016/S0167-7012(01)00370-0

Bergkemper, F., Schöler, A., Engel, M., Lang, F., Krüger, J., Schloter, M., et al. (2016). Phosphorus depletion in forest soils shapes bacterial communities towards phosphorus recycling systems. *Environ. Microbiol.* 18, 1988–2000. doi: 10.1111/1462-2920.13188

Blakemore, L. C., Searle, P. L., and Daly, B. K. (1987). Methods for chemical analysis of soils. *NZ Soil Bur Sci. Rep.* 80, 31–45. doi: 10.7931/DL1-SBSR-80

Blombäck, K., Bolster, C. H., Lindsjö, A., Hesse, K., Linefur, H., and Parvage, M. M. (2021). Comparing measures for determination of phosphorus saturation as a method to estimate dissolved P in soil solution. *Geoderma* 383:114708. doi: 10.1016/j.geoderma.2020.114708

Bramble, D. S. E., Ulrich, S., Schöning, I., Mikutta, R., Brandt, L., Poll, C., et al. (2024). Formation of mineral-associated organic matter in temperate soils is primarily controlled by mineral type and modified by land use and management intensity. *Glob. Change Biol.* 30:e17024. doi: 10.1111/gcb.17024

Brandt, L., Poll, C., Ballauff, J., Schrumpf, M., Bramble, D. S., Schöning, I., et al. (2024). Mineral type versus environmental filters: What shapes the composition and functions of fungal communities in the mineralosphere of forest soils? *Soil Biol. Biochem.* 190:109288. doi: 10.1016/j.soilbio.2023.109288

Brödlin, D., Kaiser, K., and Hagedorn, F. (2019). Divergent patterns of carbon, nitrogen, and phosphorus mobilization in forest soils. *Front. For. Glob. Change* 2:66. doi: 10.3389/ffgc.2019.00066

Brucker, E., and Spohn, M. (2019). Formation of soil phosphorus fractions along a climate and vegetation gradient in the Coastal Cordillera of Chile. *CATENA* 180, 203–211. doi: 10.1016/j.catena.2019.04.022

Brucker, E., Kernchen, S., and Spohn, M. (2020). Release of phosphorus and silicon from minerals by soil microorganisms depends on the availability of organic carbon. *Soil Biol. Biochem.* 143:107737. doi: 10.1016/j.soilbio.2020.107737

Carter, M. R., and Gregorich, E. G. (eds) (2008). *Soil Sampling and Methods of Analysis*, 2nd Edn. Boca Raton, FL: Canadian Society of Soil Science.

Celi, L., Lamacchia, S., Marsan, F. A., and Barberis, E. (1999). Interaction of inositol hexaphosphate on clays: Adsorption and charging phenomena. *Soil Sci.* 164, 574–585. doi: 10.1097/00010694-199908000-00005

Chen, A., and Arai, Y. (2019). Functional group specific phytic acid adsorption at the ferrihydrite–water interface. *Environ. Sci. Technol.* 53, 8205–8215. doi: 10.1021/acs.est.9b01511

Cornell, R. M., and Schwertmann, U. (2003). *The Iron Oxides: Structure, Properties, Reactions, Occurrences and Uses*. New York, NY: Wiley-VCH Verlag.

D'Amico, M., Almeida, J. P., Barbieri, S., Castelli, F., Sgura, E., Sineo, G., et al. (2020). Ectomycorrhizal utilization of different phosphorus sources in a glacier forefront in the Italian Alps. *Plant Soil* 446, 81–95. doi: 10.1007/s11104-019-04342-0

Darch, T., Blackwell, M. S. A., Hawkins, J. M. B., Haygarth, P. M., and Chadwick, D. (2014). A meta-analysis of organic and inorganic phosphorus in organic fertilizers, soils, and water: Implications for water quality. *Crit. Rev. Environ. Sci. Technol.* 44, 2172–2202. doi: 10.1080/10643389.2013.790752

Fetzer, J., and Hagedorn, F. (2021). *Phosphorus and Nitrogen Leaching from Beech Forest Soils*. Birmensdorf: EnviDat (Swiss Federal Institute for Forest, Snow and Landscape Research WSL). doi: 10.16904/envidat.234

Ganta, P. B., Morshedizad, M., Kühn, O., Leinweber, P., and Ahmed, A. A. (2021). The binding of phosphorus species at goethite: A joint experimental and theoretical study. *Minerals* 11:323. doi: 10.3390/min11030323

Giaveno, C., Celi, L., Richardson, A. E., Simpson, R. J., and Barberis, E. (2010). Interaction of phytases with minerals and availability of substrate affect the hydrolysis of inositol phosphates. *Soil Biol. Biochem.* 42, 491–498. doi: 10.1016/j.soilbio.2009.12.002

Göransson, H., Rosengren, U., Wallander, H., Fransson, A.-M., and Thelin, G. (2006). Nutrient acquisition from different soil depths by pedunculate oak. *Trees* 20, 292–298. doi: 10.1007/s00468-005-0034-2

Hu, H., Qian, C., Xue, K., Jörgensen, R. G., Keiluweit, M., Liang, C., et al. (2024). Reducing the uncertainty in estimating soil microbial-derived carbon storage. *Proc. Natl. Acad. Sci. U.S.A.* 121:e2401916121. doi: 10.1073/pnas.2401916121

Indorf, C., Dyckmans, J., Khan, K. S., and Joergensen, R. G. (2011). Optimisation of amino sugar quantification by HPLC in soil and plant hydrolysates. *Biol. Fertil. Soils* 47, 387–396. doi: 10.1007/s00374-011-0545-5

Joergensen, R. G. (2018). Amino sugars as specific indices for fungal and bacterial residues in soil. *Biol. Fertil. Soils* 54, 559–568. doi: 10.1007/s00374-018-1288-3

Johnson, B. B., Quill, E., and Angove, M. J. (2012). An investigation of the mode of sorption of inositol hexaphosphate to goethite. *J. Colloid Interface Sci.* 367, 436–442. doi: 10.1016/j.jcis.2011.09.066

Kleinman, P. J. A. (2017). The persistent environmental relevance of soil phosphorus sorption saturation. *Curr. Pollut. Rep.* 3, 141–150. doi: 10.1007/s40726-017-0058-4

Klotzbücher, A., Kaiser, K., Klotzbücher, T., Wolff, M., and Mikutta, R. (2019). Testing mechanisms underlying the Hedley sequential phosphorus extraction of soils. *J. Plant Nutr. Soil Sci.* 182, 570–577. doi: 10.1002/jpln.201800652

Klotzbücher, A., Schunck, F., Klotzbücher, T., Kaiser, K., Glaser, B., Spohn, M., et al. (2020). Goethite-bound phosphorus in an acidic subsoil is not available to beech (*Fagus sylvatica* L.). *Front. For. Glob. Change* 3:94. doi: 10.3389/ffgc.2020.00094

Krumina, L., Kenney, J. P. L., Loring, J. S., and Persson, P. (2016). Desorption mechanisms of phosphate from ferrihydrite and goethite surfaces. *Chem. Geol.* 427, 54–64. doi: 10.1016/j.chemgeo.2016.02.016

Lang, F., Krüger, J., Amelung, W., Willbold, S., Frossard, E., Bünemann, E. K., et al. (2017). Soil phosphorus supply controls P nutrition strategies of beech forest ecosystems in Central Europe. *Biogeochemistry* 136, 5–29. doi: 10.1007/s10533-017-0375-0

Leinemann, T., Mikutta, R., Kalbitz, K., Schaarschmidt, F., and Guggenberger, G. (2016). Small scale variability of vertical water and dissolved organic matter fluxes in sandy Cambisol subsoils as revealed by segmented suction plates. *Biogeochemistry* 131, 1–15. doi: 10.1007/s10533-016-0259-8

Leuschner, C., Hertel, D., Coners, H., and Büttner, V. (2001). Root competition between beech and oak: A hypothesis. *Oecologia* 126, 276–284. doi: 10.1007/s004420000507

Li, M., Osaki, M., Honma, M., and Tadano, T. (1997). Purification and characterization of phytase induced in tomato roots under phosphorus-deficient conditions. *Soil Sci. Plant Nutr.* 43, 179–190. doi: 10.1080/00380768.1997.10414726

Margenot, A. J., Nakayama, Y., and Parikh, S. J. (2018). Methodological recommendations for optimizing assays of enzyme activities in soil samples. *Soil Biol. Biochem.* 125, 350–360. doi: 10.1016/j.soilbio.2017.11.006

Martin, M., Celi, L., and Barberis, E. (2004). Desorption and plant availabiity of myo-inositol hexaphosphate adsorbed on goethite. *Soil Sci.* 169, 115–124. doi: 10.1097/01.ss.0000117787.98510.9d

Meier, I. C., and Leuschner, C. (2008). Genotypic variation and phenotypic plasticity in the drought response of fine roots of European beech. *Tree Physiol.* 28, 297–309. doi: 10.1093/treephys/28.2.297

Merlin, A., Rosolem, C. A., and He, Z. (2016). Non-labile phosphorus acquisition by *Brachiaria*. *J. Plant Nutr.* 39, 1319–1327. doi: 10.1080/01904167.2015.1109117

Mikutta, C., Lang, F., and Kaupenjohann, M. (2006). Citrate impairs the micropore diffusion of phosphate into pure and C-coated goethite. *Geochim. Cosmochim. Acta* 70, 595–607. doi: 10.1016/j.gca.2005.10.032

Müller, K., Kubsch, N., Marhan, S., Mayer-Gruner, P., Nassal, P., Schneider, D., et al. (2020). Saprotrophic and ectomycorrhizal fungi contribute differentially to organic P mobilization in beech-dominated forest ecosystems. *Front. For. Glob. Change* 3:47. doi: 10.3389/ffgc.2020.00047

Oliva, R. L., Khadka, U. B., Camenzind, T., Dyckmans, J., and Joergensen, R. G. (2025). Constituent of extracellular polymeric substances (EPS) produced by a range of soil bacteria and fungi. *BMC Microbiol.* 25:298. doi: 10.1186/s12866-025-04034-z

Oliva, R. L., Vogt, C., Bublitz, T. A., Camenzind, T., Dyckmans, J., and Joergensen, R. G. (2024). Galactosamine and mannosamine are integral parts of bacterial and fungal extracellular polymeric substances. *ISME Commun.* 4:ycae038. doi: 10.1093/ismeco/ycae038

Oliverio, A. M., Bissett, A., McGuire, K., Saltonstall, K., Turner, B. L., and Fierer, N. (2020). The role of phosphorus limitation in shaping soil bacterial communities and their metabolic capabilities. *mBio* 11:e01718-20. doi: 10.1128/mbio.01718-20

Osorio, N. W., and Habte, M. (2013). Phosphate desorption from the surface of soil mineral particles by a phosphate-solubilizing fungus. *Biol. Fertil. Soils* 49, 481–486. doi: 10.1007/s00374-012-0763-5

Parfitt, R. L. (1979). The availability of P from phosphate-goethite bridging complexes. Desorption and uptake by ryegrass. *Plant Soil* 53, 55–65. doi: 10.1007/BF02181879

Pastore, G., Kaiser, K., Kernchen, S., and Spohn, M. (2020). Microbial release of apatite- and goethite-bound phosphate in acidic forest soils. *Geoderma* 370:114360. doi: 10.1016/j.geoderma.2020.114360

Pautler, M. C., and Sims, J. T. (2000). Relationships between soil test phosphorus, soluble phosphorus, and phosphorus saturation in Delaware soils. *Soil Sci. Soc. Am. J.* 64, 765–773. doi: 10.2136/sssaj2000.642765x

Richardson, S. J., Peltzer, D. A., Allen, R. B., McGlone, M. S., and Parfitt, R. L. (2004). Rapid development of phosphorus limitation in temperate rainforest along the Franz Josef soil chronosequence. *Oecologia* 139, 267–276. doi: 10.1007/s00442-004-1501-y

Rodionov, A., Bauke, S. L., von Sperber, C., Hoeschen, C., Kandeler, E., Kruse, J., et al. (2020). Biogeochemical cycling of phosphorus in subsoils of temperate forest ecosystems. *Biogeochemistry* 150, 313–328. doi: 10.1007/s10533-020-00700-8

Rosenstock, N. P., Berner, C., Smits, M. M., Krám, P., and Wallander, H. (2016). The role of phosphorus, magnesium and potassium availability in soil fungal exploration of mineral nutrient sources in Norway spruce forests. *New Phytol.* 211, 542–553. doi: 10.1111/nph.13928

Santoro, V., Schiavon, M., and Celi, L. (2024). Role of soil abiotic processes on phosphorus availability and plant responses with a focus on strigolactones in tomato plants. *Plant Soil* 494, 1–49. doi: 10.1007/s11104-023-06266-2

Schreider, K., Hofmann, D., Boy, J., Andrino, A., Fernandes Figueiredo, A., Sauheitl, L., et al. (2022). Mycorrhizal mediated partitioning of phosphorus: Ectomycorrhizal (*Populus* x *canescens* x *Paxillus involutus*) potential to exploit simultaneously organic and mineral phosphorus sources. *Front. Soil Sci.* 2:865517. doi: 10.3389/fsoil.2022.865517

Spohn, M. (2024). Preferential adsorption of nitrogen- and phosphorus-containing organic compounds to minerals in soils: A review. *Soil Biol. Biochem.* 194:109428. doi: 10.1016/j.soilbio.2024.109428

Stahr, S., Graf-Rosenfellner, M., Klysubun, W., Mikutta, R., Prietzel, J., and Lang, F. (2018). Phosphorus speciation and C:N:P stoichiometry of functional organic matter fractions in temperate forest soils. *Plant Soil* 427, 53–69. doi: 10.1007/s11104-017-3394-7

Tabatabai, M. A., and Bremner, J. M. (1969). Use of p-nitrophenyl phosphate for assay of soil phosphatase activity. *Soil Biol. Biochem.* 1, 301–307. doi: 10.1016/0038-0717(69)90012-1

Turner, B. L., Condron, L. M., Richardson, S. J., Peltzer, D. A., and Allison, V. J. (2007). Soil organic phosphorus transformations during pedogenesis. *Ecosystems* 10, 1166–1181. doi: 10.1007/s10021-007-9086-z

Twieg, B. D., Durall, D. M., and Simard, S. W. (2007). Ectomycorrhizal fungal succession in mixed temperate forests. *New Phytol.* 176, 437–447. doi: 10.1111/j.1469-8137.2007.02173.x

Uhlig, D., and von Blanckenburg, F. (2019). How slow rock weathering balances nutrient loss during fast forest floor turnover in montane, temperate forest ecosystems. *Front. Earth Sci.* 7:159. doi: 10.3389/feart.2019.00159

Vitousek, P. M., Porder, S., Houlton, B. Z., and Chadwick, O. A. (2010). Terrestrial phosphorus limitation: Mechanisms, implications, and nitrogen–phosphorus interactions. *Ecol. Appl.* 20, 5–15. doi: 10.1890/08-0127.1

Walker, T. W., and Syers, J. K. (1976). The fate of phosphorus during pedogenesis. *Geoderma* 15, 1–19. doi: 10.1016/0016-7061(76)90066-5

Werner, F., de la Haye, T. R., Spielvogel, S., and Prietzel, J. (2017). Small-scale spatial distribution of phosphorus fractions in soils from silicate parent material with different degree of podzolization. *Geoderma* 302, 52–65. doi: 10.1016/j.geoderma.2017.04.026

White, T. J., Bruns, T., Lee, S., and Taylor, J. (1990). "Amplification and direct sequencing of fungal ribosomal RNA genes for phylogenetics," in *PCR Protocols: A Guide to Methods and Applications*, eds M. A. Innis, D. H. Gelfand, J. J. Sninsky, and T. J. White (San Diego, CA: Academic Press), 315–322. doi: 10.1016/B978-0-12-372180-8.50042-1

Yan, Y., Koopal, L. K., Liu, F., Huang, Q., and Feng, X. (2015). Desorption of myo-inositol hexakisphosphate and phosphate from goethite by different reagents. *J. Plant Nutr. Soil Sci.* 178, 878–887. doi: 10.1002/jpln.201500254

Yan, Y., Wan, B., Jiang, R., Wang, X., Wang, H., Lan, S., et al. (2023). Interactions of organic phosphorus with soil minerals and the associated environmental impacts: A review. *Pedosphere* 33, 74–92. doi: 10.1016/j.pedsph.2022.08.001

Yanai, R. D. (1992). Phosphorus budget of a 70-year-old northern hardwood forest. *Biogeochemistry* 17, 1–22. doi: 10.1007/BF00002757

Zavišiæ, A., Yang, N., Marhan, S., Kandeler, E., and Polle, A. (2018). Forest soil phosphorus resources and fertilization affect ectomycorrhizal community composition, bech P uptake efficiency, and photosynthesis. *Front. Plant Sci.* 9:463. doi: 10.3389/fpls.2018.00463